



ELECTRONIC DEPARTEMENT
CENTRE DE DÉVELOPPEMENT DES TECHNOLOGIES AVANCÉES

In partial fulfillment of requirement for
Engineer's Degree

Theme:

**Implementation of Source Localization Algorithms
and Application in Real Environment with
LabVIEW software and NI USRP platforms**

Yassamina BERKANE
Hinda KHELLOUF

Supervised by

Prof. Adel BELOUHRANI

Mr. Soufiane TEBACHE

Presented in public on : June 21st 2018

Jury members:

President	M. C. LARBES	Professeur	ENP
Examiner	M. M. ADNANE	Phd	ENP
Supervisors	M. A. BELOUHRANI	Professeur	ENP
	M. S. TEBACHE	Magister	ENP



ELECTRONIC DEPARTEMENT
CENTRE DE DÉVELOPPEMENT DES TECHNOLOGIES AVANCÉES

In partial fulfillment of requirement for
Engineer's Degree

Theme:

**Implementation of Source Localization Algorithms
and Application in Real Environment with
LabVIEW software and NI USRP platforms**

Yassamina BERKANE
Hinda KHELLOUF

Supervised by

Prof. Adel BELOUHRANI

Mr. Soufiane TEBACHE

Presented in public on : June 21st 2018

Jury members:

President	M. C. LARBES	Professeur	ENP
Examiner	M. M. ADNANE	Phd	ENP
Supervisors	M. A. BELOUHRANI	Professeur	ENP
	M. S. TEBACHE	Magister	ENP

Dedication

"I would like to offer this work to my dear mother, who always has been there for me during my entire curriculum. I would like to dedicate this work to my father also, who is a great source of inspiration for us, who took care of us during all these years. I would like to mention my little sister KHAOULA and my little brothers Ayoub and Lyes Imad and my grand-mother, not to forget all of my friends in POLYTECH and outside."

"To all my family, my friends and my teachers"

,Hinda KHELLOUF

"This work is for everyone that supported me, beginning with my mother and my father: who took care of me since my childhood till this day. This work is for my siblings: may they accomplish much more than this. I would like to dedicate this work to all of my family and finally, I would like to thank all my friends whom I met at every stage of my education, and every stage of my life"

"To my teachers and all my family"

"To all my dears"

,Yassamina BERKANE

Acknowledgment

*“We would like to thank our mentor, **Professor Adel Belouchrani** for guiding and supporting us over the graduate period. He has set an example of excellence as a researcher, advisor and instructor.”*

*“ We would like to offer our sincere gratitude to **Mr Soufiane TEBACHE** ,who made his great expertise in the field available to us at a moment’s notice and replied to every single question we had with great passion and in exquisite detail, for his valuable help and his availability throughout this thesis, not to mention sharing his knowledge and experience openly with us. He allowed us to increase our knowledge in electronics.”*

*“ We would like also to thank **Mr Ali MANSOUL** for his availability, his precious advice during the thesis, we learned a great deal from him, not to forget his good humor and kindness. Our sincere thanks to the committee members for reviewing our thesis and for their advice and insightful comments. ”*

الملخص

تقدير اتجاه الوصول هو أمر في غاية الأهمية في الشبكات اللاسلكية، الرادار وتطبيقات رصد مواقع الأهداف. اعتمدنا خلال هذه الدراسة على طريقتين مختلفتين: الأولى هي BARTLETT المنهج المتوافق والثانية هي MUSIC تصنيف التيار المتعدد للتحقق تجريبيا في وسط حقيقي من الخوارزميات الموجودة لتقدير اتجاه الوصول القادم من هدف ما بتردد الراديو وذلك من خلال تكوين كلتا الطريقتين في برنامج LabVIEW و تنفيذهما في لوحات NI USRP.

كلمات مفتاحية: اتجاه الوصول، تردد الراديو، MUSIC, Bartlett, USRP, LabView.

Résumé - Le but de ce projet est de vérifier expérimentalement des algorithmes dans un environnement réel pour estimer la direction d'arrivée (DoA) d'une source RF (Radio Fréquence). Pour ce faire, nous présentons deux approches différentes: la première est Multiple Signal Classification (MUSIC) et la seconde est l'estimation conventionnel de la direction de l'angle du signal (Bartlett), les deux approches sont implémentées sur des plateformes NI USRP de National Instruments . et configurer dans le logiciel LabView.
Mots-clés : direction d'arrivée, estimation, Radio Fréquence, MUSIC, Bartlett, USRP, LabView.

Abstract - The aim of this project is to present an experimental verification in real environment of algorithms to estimate direction of arrival (DOA) of an incident RF (Radio Frequency) source. To do so, we present two different approaches, The first is multiple signal classification (MUSIC) and the second is a conventionnel estimation of signal angle direction (Bartlett) , both approaches are implemented on a National Instruments (NI) USRP platforms, and the algorithms are setup in LabView NI software.
Key-words: direction of arrival, estimation, (Radio Frequency), MUSIC, Bartlett, USRP, LabView.

Contents

List of Figures

Acronyms

Introduction	15
1 Localization problem and literature solutions	17
1.1 Array Signal Processing	17
1.2 Motivation and objectives	17
1.3 Direction-of-Arrival Estimation Problem	18
1.4 Data Model	20
1.5 Array Response	21
1.6 Spectral-Based DoA Estimation Techniques	22
1.6.1 Bartlett	22
1.6.2 MUSIC	23
2 Software and Hardware Description	26
2.1 Software Defined Radio	26
2.1.1 What is Software Defined Radio SDR ?	26
2.1.2 Digital Communication System Fundamentals	26
2.1.3 Benefits and Limitations of SDR	28
2.2 Universal Software Radio Peripheral USRP	29
2.2.1 USRP and USRP RIO	29

2.3	LabView Software	34
2.3.1	LabVIEW basics	34
2.3.2	Benefits of programming in LabVIEW	35
2.3.3	LabVIEW working with NI USRP	35
2.3.4	Description of some modules in LabVIEW	37
2.3.5	Simulation of BARTLETT & MUSIC Algorithms	38
3	Setup of localization system	45
3.1	Transmitter and receivers	45
3.1.1	Transmitter	46
3.1.2	Receiver	47
3.2	Multi devices synchronization	48
3.2.1	signals of common reference	48
3.2.2	synchronization of two USRPs with MIMO cable	49
3.3	USRP RIO's channels synchronization	51
3.3.1	Phase calibration using LabVIEW module	52
3.3.2	Phase calibration using correlation	53
3.4	MUSIC & BARTLETT Algorithms implementation	54
3.4.1	Hardware Setup	57
3.4.2	Software Configuration	58
4	Localization Results and Discussions	64
4.1	Results of Implementation MuSiC and Bartlett Algorithms	64
4.1.1	Effect of the Number of Snapshots on MuSiC and Bartlett Algorithms	64
4.1.2	Effect of the Varying array spacing on MuSiC and Bartlett Algorithms	65
4.1.3	Effect of the SNR on MuSiC and Bartlett Algorithms	66
4.2	Effect of the Broadside phenomenon on MuSiC and Bartlett Algorithms .	67

4.3	Effect of the Multipath phenomenon on MuSiC and Bartlett Algorithms .	68
4.4	Indoor and Outdoor environment tests	69
4.4.1	Indoor environment test	69
4.4.2	Outdoor environment test	69
	Conclusion	74
	Bibliography	76

List of Figures

1.1	Number of the mobile cellular subscriptions from 2005 to 2010	18
1.2	The Direction-of-Arrival Estimation Problem	19
1.3	Visualization of Spatial Aliasing	20
1.4	Plane wave s_l impinging from direction-of-arrival Φ on a M-element ULA	21
1.5	N element antenna array with D arriving signals	23
2.1	Simplified Overview of a SDR	27
2.2	Digital Communication System Block Diagram	27
2.3	Typical SDR system structure	28
2.4	NI USRP platforms Identification	30
2.5	USRP 2920 Block Diagram	31
2.6	NI USRP RIO-2942- platform	32
2.7	USRP RIO Architecture	33
2.8	RIO datasheet	34
2.9	Typical LabVIEW VI	34
2.10	Basic steps of controlling USRP via LabVIEW	36
2.11	The eight most-used NI-USRP functions	36
2.12	Example front panel for USRP receiver	37
2.13	Example block diagram for USRP receiver	37
2.14	Block Diagram of Bartlett's algorithm test	39
2.15	Block Diagram of Generation module	40

2.16	Diagram of Direction vector	41
2.17	BARTLETT Algorithm steps	41
2.18	Bartlett Beam block diagram	42
2.19	Front panel of BARTLETT algorithm with 2 sensors	42
2.20	Front panel of BARTLETT algorithm with 10 sensors	43
2.21	Music Algorithm Steps	43
2.22	Block diagram of Estimating Noise Space	43
2.23	Diagram of MUSIC algorithm processing	43
2.24	Front panel of MuSiC algorithm with 2 sensors	44
2.25	Front panel of MUSIC algorithm with 10 sensors	44
3.1	Generic communication system	45
3.2	Block diagram of Sinus transmitter	46
3.3	Block diagram of Sine Generation module	47
3.4	TX front panel tool	47
3.5	Baseband power spectrum of the transmitted signal	48
3.6	Block diagram of a receiver with USRP RIO card	48
3.7	Front panel of RX tool	49
3.8	Synchronization of multiple USRPs	49
3.9	USRPs receivers with MIMO cable	50
3.10	Synchronization of two USRPs with MIMO cable	50
3.11	multi-channel system calibration	52
3.12	phase compensation bloc diagram	53
3.13	Phase shift before and after phase calibration Front Panel	53
3.14	Multi channel cabled system for Correlation method phase detection	54
3.15	Phase shift using MATLAB script	54
3.16	Phase shift using FFT method	54

3.17	Phase shift using LabVIEW module	54
3.18	Received graph before synchronization	55
3.19	Graph of the signal after phase synchronization	55
3.20	Baseband Power spectrum of the received graph	55
3.21	The three phase shift detected	56
3.22	Cross correlation graph of the two components of the received signal	56
3.23	The DoA Detection System with USRP RIO and USRP Hardware Setup Diagram	57
3.24	The AoA Detection System with USRP RIO and USRP Hardware Setup Diagram	58
3.25	Target Source transmitter IQ graph front panel	58
3.26	Target Source transmitter baseband power spectrum graph front panel	58
3.27	Target Source Transmitter Block Diagram	59
3.28	Receiver VI front panel	60
3.29	USRP hardware configuration block	60
3.30	receiver IQ graph front panel	60
3.31	USRP control Block	61
3.32	Block diagram of baseband signal processing	62
3.33	Implementation of Music Algorithm with Matlab block diagram	62
3.34	Implemetation of BArtlett Algorithm with Matlab block diagram	62
3.35	Implementation of MuSiC Algorithm using LabVIEW Functions	63
3.36	Implementation of Bartlett Algorithm using LabVIEW Functions	63
4.1	MuSiC with 10 snapshots	65
4.2	MuSiC with 200 snapshots	65
4.3	MuSiC with 16384 snapshots	65
4.4	Bartlett 10 snapshots	65
4.5	Bartlett 200 snapshots	65

4.6	Bartlett 16384 snapshots	65
4.7	MuSiC ($d=\lambda$)	66
4.8	MuSiC ($d=\lambda/2$)	66
4.9	MuSiC ($d=\lambda/4$)	66
4.10	BARTLETT ($d=\lambda$)	66
4.11	BARTLETT ($d=\lambda/2$)	66
4.12	Bartlett ($d=\lambda/4$)	66
4.13	MuSiC SNR=-20dB	67
4.14	MuSiC SNR=-10dB	67
4.15	MuSiC SNR= 0 dB	67
4.16	Bartlett SNR=-20dB	67
4.17	Bartlett SNR=-10dB	67
4.18	Bartlett SNR=0dB	67
4.19	Broadside -70 degrees	68
4.20	MUSIC broadside -70	68
4.21	Bartlett broadside -70	68
4.22	broadside angle 90 degrees	69
4.23	MUSIC broadside 90	69
4.24	Bartlett broadside 90	69
4.25	Indoor test 0 degree	70
4.26	MuSiC indoor detection 0	70
4.27	Bartlett indoor detection 0	70
4.28	Indoor test -45 degree	71
4.29	MuSiC indoor detection -45	71
4.30	Bartlett indoor detection -45	71
4.31	Outdoor test 0 degrees	72

4.32 MuSiC indoor detection 0	72
4.33 Bartlett indoor detection 0	72
4.34 Outdoor test -45 degrees	73
4.35 MuSiC indoor detection -45	73
4.36 Bartlett indoor detection -45	73

Acronyms

ADC	A nalog-to- D igital C onverter
AWGN	A dditive W hite G aussian N oise
BPF	B and P ass F ilter
DAC	D igital-to- A nalog C onverter
DC	D igital C urrent
DDC	D igital D own C onverter
DoA	D irection of A rrival
DSP	D igital S ignal P rocessing
DUC	D igital U p C onverter
FFT	F ast F ourier T ransform
FIR	F inite I mpulse R esponse
FPGA	F ield P rogrammable G ate A rray
GUI	G raphical U ser I nterface
I	I n-phase
IIR	I nfinite I mpulse R esponse
IF	I ntermediate F requency
I/Q	I n-phase/ Q uadrature
LNA	L ow N oise A mplifier
LO	L ocal O scillator
LP	L ow P ass
LPF	L ow P ass F ilter

Acronyms

MIMO	M ultiple I nter M ultiple O utput
MUSIC	M ultiple S ignal C lassification
NI	N ational I nstruments
OFDM	O rthogonal F requency D ivision M ultiplexing
PC	P ersonal C omputer
Q	Q uadrature
RF	R adio F requency
RX	R eceiver side
SDR	S oftware D efined R adio
SNR	S ignal to N oise R atio
TX	T ransmitter side
ULA	U niform L inear A rray
USB	U niversal S erial B us
USRP	U niversal S oftware R adio P eripheral
USRP RIO	U niversal S oftware R adio P eripheral R econfigurable I nterface O utput
VCO	V oltage C ontrolled O scillator
VI	V irtual I nstrument

Introduction

DOA estimation plays an important role in array signal processing, and has a wide range of application. In this work, We will describe DOA estimation, and give its mathematical model.

Then estimate DOA based on the MUSIC and BARTLETT algorithms, and also give some simulations with MATLAB and implement it in LabVIEW to simulate what factors can affect their accuracy and resolution.

Estimating the Direction of Arrival of an incident source signal is an active research area due to its innumerable applications in radar, sonar for source localization, and beam-forming/steering in mobile communication.

A number of techniques has been proposed and validated in simulations to improve the performance of DoA systems. However, validation of those techniques in actual hardware is much more challenging because implementing such a system in hardware takes a significant amount of time, effort and with a high cost. Currently, the Software Defined Radio approach could help researchers and engineers to reduce the time, effort and cost to implement a localization system. Thus, SDR approach is widely spread in designing localization systems. The use of SDR enables to transform radio hardware problems into software problems.

Moreover, a significant amount of signal processing can be conducted in software. This platform offers great flexibility to researchers and developers to design new protocols, methods or techniques for localization and wireless communication systems. LabVIEW software and USRP hardware are the common platforms used in SDR systems.

The advantages of SDR platform discussed above motivate us to implement Source localization system using Laboratory Virtual Instrument Engineering Workbench (LabVIEW) software and Universal Software Radio Peripheral (USRP) hardware platform. Precisely, we used LabVIEW 15.0 development system software and the National Instrument's (NI) USRP-2942R and USRP-2921 hardware. For presenting two different approaches to estimate direction of arrival (DOA) of an incident RF source. In one hand, the first proposed method is Multiple Signal Classification (MUSIC) which is based on extracting the signal and noise subspaces from the R matrix received data matrix. The angle of the signal arrival is extracted from the signal subspace. In the other hand, Beam-forming method conventional beamformer with (BARTLETT) algorithm.

The DOA estimators is tested in both indoor space in the lab and open atmosphere. The experiment setup and measurement results show that the DOA of incoming sources can be successfully estimated in different realistic scenarios and in real time.

The report is organized as follows. The first Chapter gives an introduction to localization problem and literature solutions as to know what is expected from our system. The second chapter discusses the used Software and Hardware. The experimental setup and procedures are discussed in details in Chapter 3 followed by the experimental results and discussion in chapter 4, We sum up the report by a conclusion.

Chapter 1

Localization problem and literature solutions

1.1 Array Signal Processing

In literature, sensor array signal processing, array signal processing or simply array processing are three terms that refer to a field of signal processing that uses a group of sensors arrayed in a particular geometry to estimate a signals parameters and extract it in the presence of noise using its temporal and spatial characteristics.

There are three traditional problems related to array processing:

- Detection which is finding the number of emitting sources (M).
- Estimation which is concerned with estimating the DOA of these sources.
- Reception or beamforming which is the isolation of the desired signal and suppressing the interference by multiplying the received signal $x(t)$ by a weight vector $w(t)$.

Array processing has a wide range of applications in many aspects of electrical engineering or interdisciplinary research. One of these applications is DOA estimation which is the eld of application that is investigated in this report. Another application is in communications systems such as satellite communication, 2G and following generations which use array processing to improve the system performance and to increase its capacity [1]

1.2 Motivation and objectives

DOA estimation is an important technique in the field of signal processing in which the exact location of the source can be found from incoming RF signals. This technique is used in the array signal processing for the purpose of wireless communication and audio/ speech processing systems. In the last decade, wireless communication services have known an explosive growth. According to the International Telecommunication Union (ITU), in five years the number of mobile cellular subscriptions worldwide doubled, from 2.2 billion in 2005 to a tremendous 5.3 billion in 2010. 90 percent of the world population now has access to mobile networks. There is a constant demand for cheaper and more efficient portable devices. To sustain this enormous expansion of the mobile telecommunication

market, the modern mobile technology has to evolve in like manner.

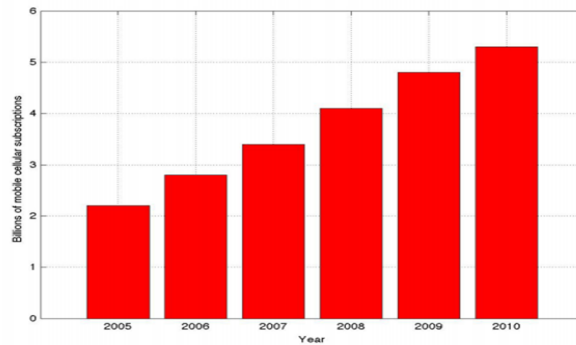


Figure 1.1: Number of the mobile cellular subscriptions from 2005 to 2010

The ever increasing number of mobile subscribers and limited available bandwidth, introduces major challenges for the wireless technology, especially in densely populated areas. Mobile communication techniques have to improve the capacity of the network and reduce co-channel interference. Over the years, a number of technologies have emerged that, very effectively, deal with these high demands. Channel access methods such as Frequency Division Multiple Access (FDMA), Time Division Multiple Access (TDMA) and Code Division Multiple Access (CDMA) allow different data streams to be transmitted in parallel over the same communication channel by dividing frequency bands and time slots and allocating different code schemes respectively. They efficaciously increase the channel throughput and avoid interference between the users. As the number of wireless users unceasingly expands and with the recent shift in emphasis from voice to multimedia applications, research towards smart antennas (SAs) emerged to attain an even higher system capacity. Smart antennas exist out of multiple antennas collaborating, forming an antenna array. The use of SAs allows the application of Space-Division Multiple Access (SDMA). SDMA spatially separates signals, i.e. based on their location and independent from their carrier frequency, time slot or assigned code. To determine the positions of the users, Direction of-Arrival (DoA) finding algorithms are used. This work concentrates on these DoA estimation algorithms. The aim of this work is to build and test in a real environment, using NI USRP platforms, a number of well known DoA estimation algorithms. Comparing their performance through simulations, and in an indoor/outdoor environment. [2]

1.3 Direction-of-Arrival Estimation Problem

The problem of interest here is estimation the DOAs of emitter signals impinging on a receiving array when a given finite data set $x(t)$ is observed over $t = 1, 2, \dots, N$ [9]

There are two research directions for DOA estimation, self-adaption array signal processing and spatial spectrum estimation. Self-adaption occurs earlier in literature than spatial spectrum and has already been used in many practical engineering systems. On the other hand, though spatial spectrum estimation has developed rapidly and had abundant references, it is rarely found in practical systems. At present, it is still being developed. Spatial spectrum is an important concept in array signal processing theory. It presents the distribution of signals in every direction in the space. Hence, if one can get the signal's spatial spectrum, one can get the direction of arrival (DOA). Consequently, spatial

spectrum estimation can be also called as DOA estimation. DOA estimation is a key research area in array signal processing and many engineering applications [3]

Consider multiple signals s_i ($i = 1, \dots, L$) impinging on a receiver from different direction of-arrivals (DoAs). We assume that these signals are plane waves arriving from a direction of-arrival ϕ_i .

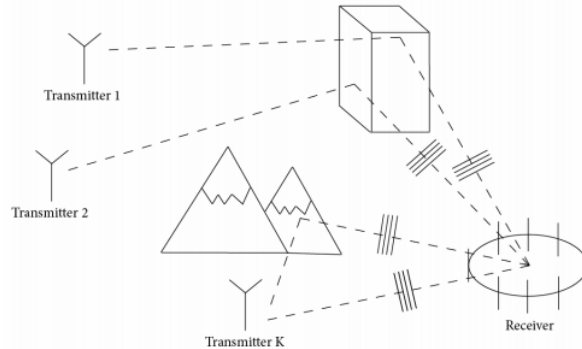


Figure 1.2: The Direction-of-Arrival Estimation Problem

The impinging signals can be either reflections – delayed copies from the same signal – or signals arriving from different transmitters. When the receiver is able to properly estimate the DoAs of the received signals using a smart antenna system, it can direct its antenna beam in these angles. It thus improves considerably the efficiency of the reception.

There are several problems the receiver has to deal with, while estimating the angles of-arrival.

Firstly the communication channel is introducing noise.

Secondly the waves arriving from different angles-of-arrival can have unequal amplitudes, which sometimes makes it difficult to distinguish between an actual and an interfering signal.

Another difficulty is reflection, which causes signals to be highly correlated and – if not properly treated – causes the DoA estimation algorithms to produce misleading results.

An additional complication is that the receiver is unaware of the number of signals that are impinging.

Moreover, the receiver has to cope with it's own imperfections, e.g. mutual coupling of the channels, their phase unsynchronization, sensor position errors or platform effects.

Then, The practical applications of Signal-Subspace techniques have been limited due to the fact that calibration errors relating to the electrical and/or geometrical characteristics of the array, can severely degrade their performance, this leads to deal with Array calibration problem.[4]

Finally, the problem of spatial aliasing, It is well known fact from the sampling theorem that aliasing occurs in the frequency domain if the signal is not sampled at high enough rate (the minimum rate is Nyquist sampling rate given by the twice of the bandwidth of the signal).

We have the same sort of considerations to take into account when we analyze the spectrum of the spatial frequency as well. The Nyquist equivalent of the sampling rate to avoid spatial aliasing implies that the distance between the sensors d should be less than or equal to the half of the minimum wavelength , i.e, $d \leq \frac{\lambda_{min}}{2}$ where λ_{min} is the mini-

imum wavelength corresponding to the maximum frequency f_{max} . This is due to the fact that the velocity of sound, $v = f\lambda$ is fixed in a medium and thus, when the frequency is maximum, the wavelength is minimum.

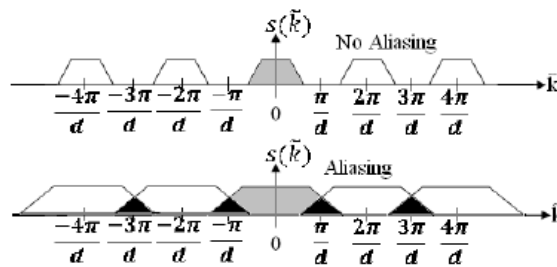


Figure 1.3: Visualization of Spatial Aliasing

In Figure 1.3 \tilde{k} is the space domain or wavenumber. whereas $s(\tilde{k})$ is the sampled signal in space domain. In the top of the Figure Nyquist Sampling Rate is maintained and as a result there is no overlap of the spectra of the sampled signals but in the bottom of the Figure aliasing occurs as Nyquist criterion is not maintained.[5]

1.4 Data Model

We consider an M-element uniform array on which signals $s_1(t), s_2(t), \dots, s_L(t)$ are incident from L different DoAs (1;2;...;L). We write for the received signal - the array data

$$X(\Phi, t) = \begin{bmatrix} X_1(\Phi, t) \\ X_2(\Phi, t) \\ \vdots \\ X_M(\Phi, t) \end{bmatrix} = A(\Phi)S(t) + N(t)$$

where $A \in C(M \times L)$ is the array response matrix, $S(t) \in C(L \times 1)$ the matrix containing the impinging signals and $N \in C(M \times 1)$ is the noise matrix. Under the assumption that the incident signals and the noise are uncorrelated the signal correlation matrix can be represented as

$$R_x = A(\phi)R_s A^H(\phi) + \sigma_n^2 I_M \quad (1.1)$$

where R_s is the signal correlation matrix, σ^2 the noise power at each array element and I_M a $M \times M$ identity matrix. To estimate R_x we compute

$$\widehat{R}_x = \frac{1}{T} X_M X_M^H \quad (1.2)$$

Where T denotes the number of samples.

1.5 Array Response

Consider the case of a M -element uniform linear array on which a plane wave s_l impinges from a direction-of-arrival Φ_l .

Under farfield assumptions, we write for the time delay τ_m between a reference element - element 1 in Figure 1.4 and the m -th element in the array

$$\tau_M = (m - 1) \frac{d_x \cos(\Phi_1)}{c} \quad (1.3)$$

where c is the speed of light and d_x the inter-element distance.

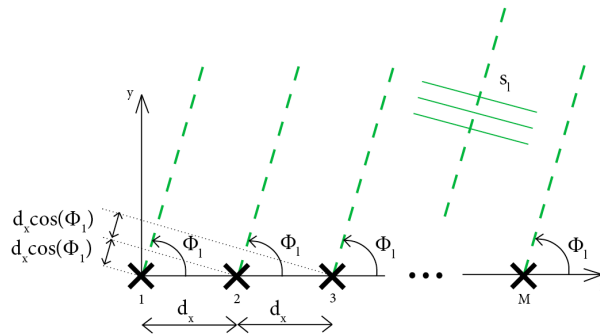


Figure 1.4: Plane wave s_l impinging from direction-of-arrival Φ_l on a M -element ULA

Now we can write the antenna array response $A(\Phi)$ to the impinging plane wave s_l as

$$A(\Phi) = \begin{bmatrix} a_1(\Phi_1) & a_2(\Phi_2) & \cdots & a_L(\Phi_L) \end{bmatrix}$$

$$a_l(\Phi_l) = \begin{bmatrix} 1 & e^{-jk d_x \cos(\Phi_l)} & e^{-j2k d_x \cos(\Phi_l)} & \cdots & e^{-j(M-1)k d_x \cos(\Phi_l)} \end{bmatrix}^T$$

where $a_l(\Phi)$ is the response of the l -th antenna element and k is the wavenumber of the plane wave.

- We write for the noise matrix

$$\mathbf{N} = \begin{bmatrix} n_1 & n_2 & \cdots & n_N \end{bmatrix}^T$$

We assume the noise components to be Additive White Gaussian Noise (AWGN). This models the background noise of the communication channel.

1.6 Spectral-Based DoA Estimation Techniques

We can subdivide the direction-of-arrival estimation methods into two main groups. We distinguish between low resolution and High resolution DoA estimators. Spectral-based DoA estimation techniques will estimate the mean power P in function of the look angle Φ . It then estimates the DoAs by determining the local maxima in the power spectrum $P(\Phi)$. We discuss two spectral-based DoA estimation methods, starting with the Bartlett procedure. Finally we introduce MUSIC estimator which belong respectively to a low resolution and high resolution algorithms.

1.6.1 Bartlett

One of the earliest methods of spectral analysis of DOAs is the Bartlett method. The idea is to guide the antenna beam in one direction (by using weighting vector $w(t)$ which acts like a spatial filter) and measure the output power. The directions which result in maximum power yield the DOA estimated.[6]

We can express the Bartlett estimation technique by the following formula

$$P_{\Phi} = A^H(\phi)R_x A(\phi) \quad (1.4)$$

where $A(\Phi)$ is the antenna array response, R_x is the signal correlation matrix and H is an operator denoting the hermitian transpose. Bartlett suffers from poor resolution, which can only be increased by increasing the number of antenna array elements which is a fairly expensive technique and thus undesired for. Also, Bartlett faces spectral leakage problems. If an antenna array is steered in a direction Φ , the array not only measures the mean power P from signals arriving from that direction Φ , but it also measures the power of signals arriving from directions other than Φ albeit with a strong attenuation. This effect, which is undesired for, can be prevented by making use of special weighing techniques. This however decreases the resolution of the Bartlett estimator. An important advantage that the Bartlett DoA estimation method has over other DoA estimation techniques, is that it's resolution is independent from the signal-to-noise-ratio (SNR) in the communication channel. [2]

1.6.2 MUSIC

MUSIC is an acronym which stands for Multiple Signal classification algorithm was developed for the first time by Schmidt in 1979 and this higher resolution technique is based on exploiting the eigen-structure of input covariance matrix. This method is to decompose the covariance matrix into eigenvectors in both signal and noise subspaces. The direction of sources is calculated from steering vectors orthogonal to the noise subspace. Which detect the peak in spatial power spectrum [5].

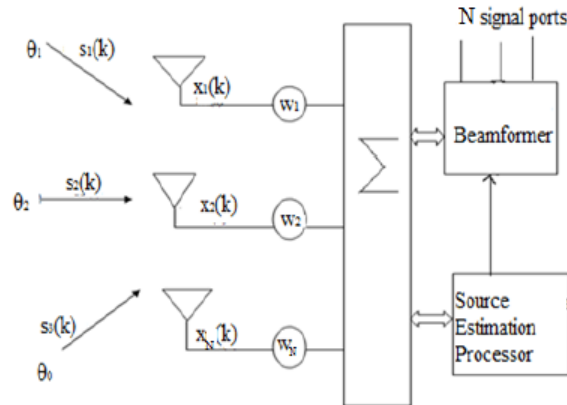


Figure 1.5: N element antenna array with D arriving signals

The implementation of the MUSIC algorithm is as follow:

- 1- In the first step the estimation of the input covariance matrix is based on N received signal vector.
 - 2- The second important step is to find the eigenvalue calculated by decomposing the covariance matrix.
 - 3- The eigenvalue is calculated and then according to order of Eigenvalues take that eigenvector and eigenvalue which are equal to number of signal D as and take that as a part of space.
 - 4- The remaining M-D eigenvectors and eigenvalues are taken as a part of noise. [10]
 - 5- Compute the MUSIC spectrum.
 - 6- In the last step spectrum function is calculated and the estimated value of DOA is found by searching the peak values. [10]
- If D is the number of signal eigenvalues or eigenvectors and the number of noise eigenvalues

or eigenvectors is N-D, the array correlation matrix with uncorrelated noise and equal variances is than given by:

$$R_{xx} = AR_{ss}A^H + \sigma_n^2 I_M \quad (1.5)$$

Where

$A = \begin{bmatrix} a(\Phi_1) & a(\Phi_2) & a(\Phi_3) & \dots & a(\Phi_D) \end{bmatrix}^T$ is (N x D) array steering matrix

$R_{ss} = \begin{bmatrix} s_1(k) & s_2(k) & s_3(k) & \dots & s_D(k) \end{bmatrix}^T$ is (D x D) source correlation matrix

R_{xx} has D eigenvectors associated with signals and (N - D) eigenvectors are associated with noise, we can then construct the N x (N-D) subspace spanned through the noise eigenvectors such that

$$V_N = \begin{bmatrix} V_1 & V_2 & V_3 & \dots & V_{N-D} \end{bmatrix}$$

The noise subspace eigenvectors are orthogonal to array steering vectors at the angles of arrivals $\Phi_1, \Phi_2, \Phi_3, \dots, \Phi_D$ and Pseudospectrum of the MUSIC given as:

$$P_{MUSIC}(\Phi) = \frac{1}{\text{abs}(a(\Phi)^H V_N V_N^H a(\phi))} \quad (1.6)$$

However when signal sources are coherent or noise variances vary the resolution of MUSIC diminishes, we must collect many time samples of received signal plus noise; we assume ergodicity and estimate the correlation matrices via time averaging as:

$$R_{xx} = \frac{1}{\sum X(k)X^H(k)}$$

$$R_{xx} = AR_{ss}A^H + AR_{sn} + R_{ns}A^H + R_{nn}$$

The MUSIC Pseudospectrum using equation with time averages now provides high angular resolution for coherent signals. MUSIC's Spatial Spectrum

$$P_{MUSIC} = \frac{1}{a^H(\Phi)E_nE_n^Ha(\Phi)} \quad (1.7)$$

Where $a(\Phi)$ is steering vector and E_n is noise subspace eigenvectors.

The DOA estimates are obtained by scanning the angle ϕ in the range $[-90; 90]$ and observing peaks of the spatial spectrum function $S(\theta)$. [7]

The MUSIC algorithm is only for the spatial spectrum estimation of incoherent signals. When signal sources are coherent, the coherent signals will unite into one signal, then the independent signal sources that received by the array will decrease, which lead to the array covariance matrix rank reduce and the number of larger eigenvalues less than the incoming signal. Spatial spectral curve does not present the peak, thus cannot obtain the correct signal DOA estimation [8]

Chapter 2

Software and Hardware Description

2.1 Software Defined Radio

2.1.1 What is Software Defined Radio SDR ?

Software Defined Radio (SDR) is defined as:“Radio in which some or all of the physical layer functions are software defined.”

SDR refers to the technology wherein software modules running on a generic hardware platform are used to implement radio functions. Combine the NI USRP hardware with LabVIEW software for the flexibility and functionality to deliver a platform for rapid prototyping involving physical layer design, wireless signal record & playback, signal intelligence, algorithm validation, and more.

A software-defined radio system is a radio communication system in which certain hardware components are implemented in software. These hardware components include filters, amplifiers, modulators, and demodulators. Because these components are defined in software, you can adjust a software-defined radio system as needed without making significant hardware changes. Since computers today may contain very fast processors and high-speed interfaces, we can leverage these abilities for our software defined radio by implementing them on a computer quickly, using LabVIEW. An overview of a SDR is depicted in Figure 2.1.

2.1.2 Digital Communication System Fundamentals

A typical digital communication system includes a transmitter, a receiver, and a communication channel. Figure 2.2 illustrates the general components of a digital communication system. The transmitter, shown as blocks on the top row, contains blocks for source and channel coding, modulation, simulating real-world signal impairments, and up

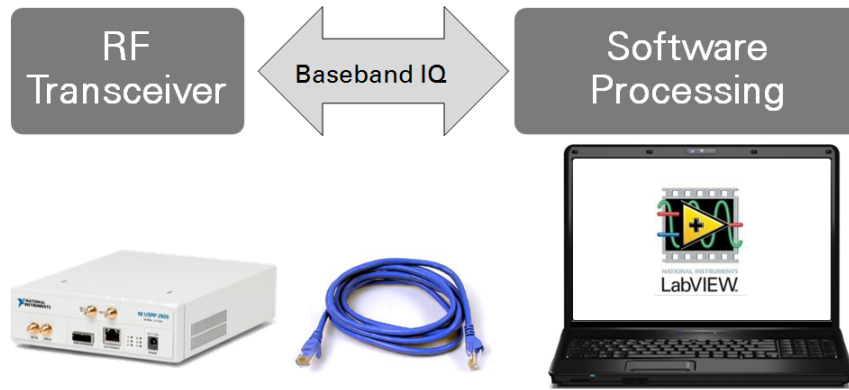


Figure 2.1: Simplified Overview of a SDR

conversion. The receiver, which includes the blocks in the bottom row, has blocks for down conversion, matched filtering, equalization, demodulation, channel decoding and source decoding.

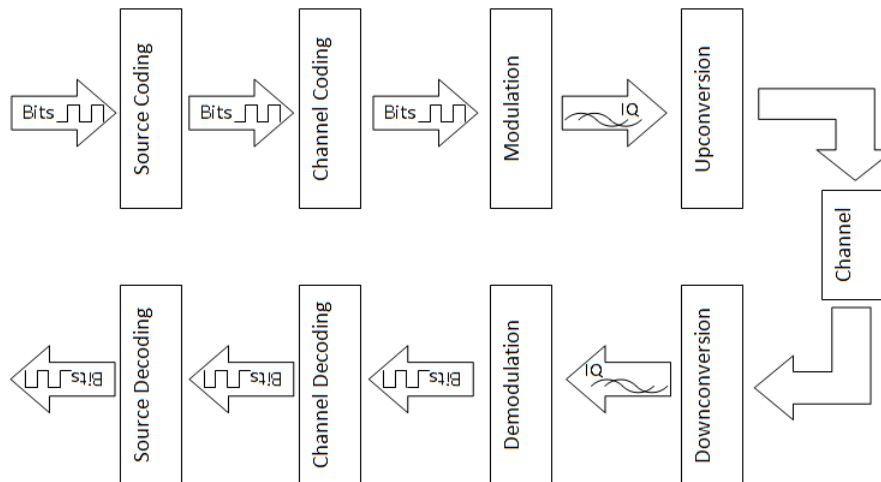


Figure 2.2: Digital Communication System Block Diagram

SDR is the concept which implements radio transmitters and receivers with programmable software instead of implementing them completely using hardware . This will provide the possibility of reconfiguring and adjusting the RF parameters in the software layer, so that the same radio hardware can work for different requirements. At the transmitter side of a typical SDR system, the SDR software transforms the data into processed digital signals with the user's preferences and provides the digital signal to digital to analog converter (DAC). The DAC transform the digital signal into analog waveforms. Afterwards the analog waveform is transmitted through the antenna to the radio channel, or through cables for precise testing purposes. At the receiver side of the SDR system, the antenna acquires the received analog waveform which is then processed by the analog front end and provided to the ADC, which transforms the analog waveform into a digital signal. The digital signal then proceeds to the SDR software for further signal processing and recovering the data that has been transmitted. The physical layer architecture of a typical current SDR system is seen in Figure 2.3 . The antennas in this system can also be SDR controlled. When the antennas are SDR controlled, the capability of the system

will be increased due to its greater tunability [11].

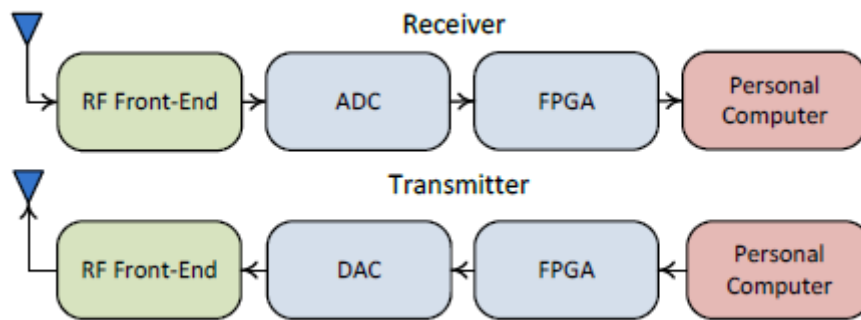


Figure 2.3: Typical SDR system structure

In the above SDR system, the RF front end is in charge of get the signal from desired carrier frequency and transfers it to a specific IF or baseband at the receiver side, or shifts the baseband signal to a desired carrier frequency at the transmitter side. ADC/DAC is used to make transformations between analog and digital signal, while digital signals are used in Field Programmable Gate Array (FPGA) and PCs, analog signals are used in RF front end and antennas. FPGAs in the SDR are embedded with specific digital signal processing codes that can perform digital baseband and RF processes, such as up/down-conversion, channelization filtering and modulation. Main calculations, system monitoring and upper layer application like spectrum analysis, radio playback, etc., are performed by the PCs [11].

2.1.3 Benefits and Limitations of SDR

Using software instead of hardware not only reduces the manufacturing cost and the maintenance time, but also allows for more flexible systems to be developed. In addition, having a processor to replace many hardware components will increase the hardware life-time until a new hardware generation is introduced [10]. If the software is well-written in such a modular manner, software re-usability and portability will be a great benefit as well. Another advantage of using SDR is the ability to create blocks in software, do simulation and test the system's behaviour before using the same software for a real-time product . Although SDR is very advantageous, unfortunately, there are few disadvantages and limitations. Disadvantages include: power consumption, efficiency and speed of hardware. For example ASICs are better in terms of these three metrics, since the designer can optimise his design to fit a specific application while GPP are aimed to be general purpose. However, SDR benefits from the rapid developments in GPP field especially, the multicore technologies and the parallel computing . SDR also has two limitations: First, LNAs have bandwidth restrictions . Second, DAC/ ADCs dynamic range, sampling rate and band-width requirements are higher than the practical capabilities . With all the advantages and disadvantages of SDR, there is still some signal processing that needs to be done on the hardware such as multirate processing and filtering. This processing is done on an FPGA [10].

2.2 Universal Software Radio Peripheral USRP

USRP is a widely used SDR platform which possess various abilities of SDR, such as wide range of bandwidth and great tunability. USRP connects real-time RF systems to PCs using Universal Serial Bus (USB) or Ethernet connections. Second generation USRPs are able to work with GNU radio, NI-Labview and Simulink. The USRP series under National Instruments' brand is called NI-USRP and are paired with NI-Labview tool boxes, which is used in the implementation of this project [11].

2.2.1 USRP and USRP RIO

NI USRPs are SDR prototype platforms capable of numerous applications for education and research. The combination of NI's hardware and software offers flexibility and functionality for physical layer design, record and playback, signal intelligence, algorithm validation, and more in affordable price.

The 2921 USRP and 2942 Rio USRP models are used for the implementation, are connected to PCs using Ethernet and PCIe x4 connections respectively working in pair with NI-LabVIEW and both are able to perform multiple input, multiple output (MIMO) functionalities. In this work, the NI USRP- Rio 2942 and NI USRP 2921 models are used for the implementation [11].

• NI USRP 2921

The National Instruments universal software radio peripheral (USRP) 2921 device can send and receive signals for use in various communications applications.

NI USRP-2921 model is shown in Figure 2.4. There are two SMA signal ports RX1/TX1 (which can perform both transmission and reception) and RX2, an Ethernet connection port, a MIMO expansion port, and an external reference clock input port, a pulse per second reference input port, and a power adapter port in the front panel. The NI USRP-2921 model has a frequency range from 2.4 GHz up to 2.5 GHz and 4.9 GHz up to 5.9 GHz with an instantaneous Real-Time bandwidth of 48 MHz (with 8 bit samples) or 24 MHz (with 16 bit samples). When the USRP works as transmitter, the DAC rate is 400 MS/s for 16 bit samples with 2 channels, and the DAC Spurious Free Dynamic Range (SFDR) is 80 dB. When it works as receiver, the noise figure is around 5 to 7 dB and the ADC rate is 100 MS/s with a SFDR of 88 dB. The maximum input power at RX is 0 dBm. More detailed information about NI USRP specifications.

In terms of hardware structure of NI USRP-2921, as seen in Figure 2.5, the RF switches are used to select which port of RX/TX to use. The TX1/RX1 port can work for both transmit and receive and the RX2 port can be only used to receive. When it works as a receiver, the analog waveform is acquired from the selected RX port and fed to low noise

NI USRP Software Defined Radio

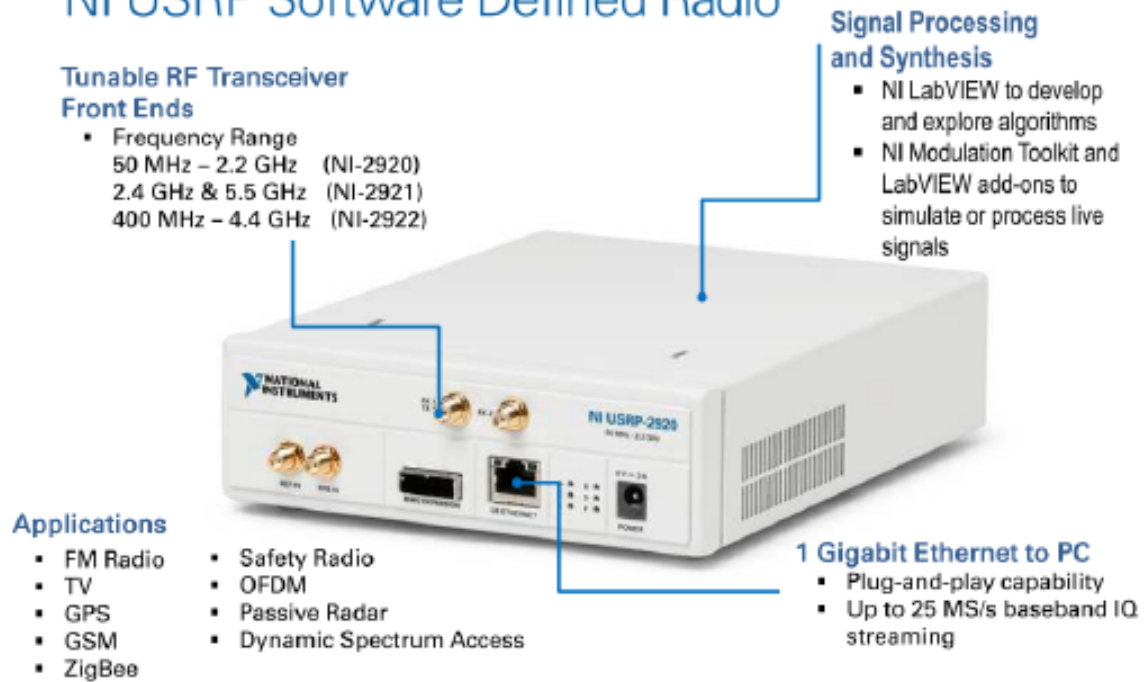


Figure 2.4: NI USRP platforms Identification

amplifier (LNA) and drive amplifier, the amplified signal is then mixed with local oscillator (LO) in order to move the signal to baseband or IF from carrier frequency. The signals (real parts and imaginary parts) are filtered by low pass filters (LPF) with bandwidth of 20 MHz and then converted into digital signal by ADC and fed to a programmable digital down converter (DDC) to perform down-conversion, if needed, and finally the digital signal is transmitted to PC via 1 Gbit Ethernet for further processing. When working as a transmitter, the processed digital signal is first transmitted from PC to USRP hardware via Ethernet and then feed to digital up converter (DUC) for up-conversion, and then the digital signal is converted into analog signal by DAC. The analog signals are then filtered by 20 MHz LPF and mixed by local oscillator in order to transfer the signal form baseband to a specific carrier frequency and then amplified according to user's preferences by the TX amplifier. The last step is to transmit the signal through TX1 to antennas or cables (the TX/RX should be correctly selected in the setting of USRP otherwise errors will occur). The NI USRP connects to a host PC to act as a software-defined radio. Incoming signals attached to the standard SMA connector are mixed down using a direct-conversion receiver (DCR) to baseband I/Q components, which are sampled by a 2-channel, 100 MS/s, 14-bit analog-to-digital converter (ADC).

The digitized I/Q data follows parallel paths through a digital down conversion (DDC) process that mixes, filters, and decimates the input 100 MS/s signal to a user-specified rate. The downconverted samples, when represented as 32-bit numbers (16 bits each for I and Q), are passed to the host computer at up to 20 MS/s over a standard Gigabit Ethernet connection.

For transmission, baseband I/Q signal samples are synthesized by the host computer and fed to the USRP-2921 at up to 20 MS/s over Gigabit Ethernet when represented with 32-bits (16-bits each for the I and Q components). The USRP hardware interpolates

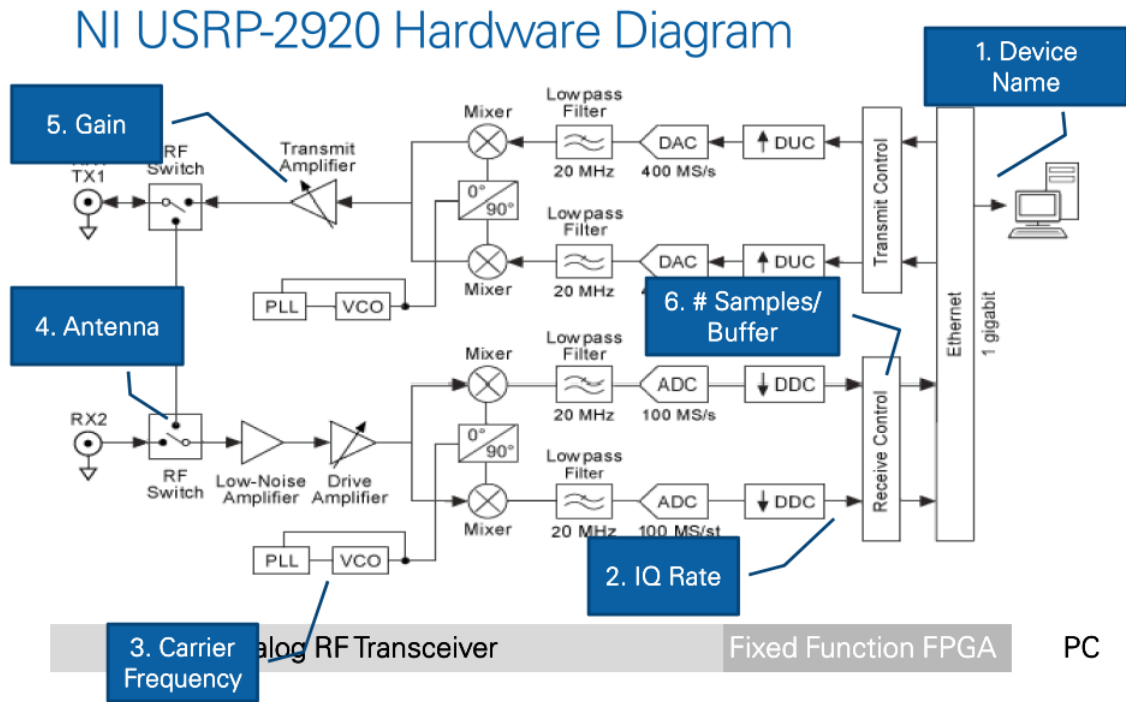


Figure 2.5: USRP 2920 Block Diagram

the incoming signal to 400 MS/s using a digital upconversion (DUC) process and then converts the signal to analog with a dual-channel, 16-bit digital to-analog converter (DAC). The resulting analog signal is then mixed up to the specified carrier frequency. An available 8-bit mode, in which 16-bits total are used to represent the I and Q values of a downconverted sample or sample to be upconverted, can enable a transfer rate of up to 40 MS/s over the Gigabit Ethernet or PCIe x4 connection between the host PC and the USRP [1].

• NI USRP RIO 2942

The USRP RIO software defined radio (SDR) platform provides an integrated hardware and software solution for rapidly prototyping high-performance wireless communication systems. Each USRP RIO device has two RF transceivers and a large Xilinx Kintex-7 (410T) FPGA in a half-1U rack-mountable form factor. The Kintex-7 FPGA is a reconfigurable LabVIEW FPGA target that incorporates DSP48 coprocessing for high-rate, low-latency applications. With the flexible hardware architecture and the LabVIEW unified design flow, researchers can prototype faster and significantly shorten time to results. A NI USRP RIO is shown in figure 2.6 Researchers around the world are using this design flow to prototype a wide range of advanced research applications that include direction finding; beamforming; multiple input, multiple output (MIMO); synchronization of heterogeneous networks; LTE relaying; RF compressive sampling; spectrum sensing and cognitive radio [10].



Figure 2.6: NI USRP RIO-2942- platform

The technical specifications of USRP units (NI USRP-2942R) used in this project are as follows [10]:

- 1.2 GHz to 6 GHz Tuneable RF Transceiver.
- Large reconfigurable DSP48 based Xilinx Kintex-7 FPGA.
- 40 MHz per channel real-time bandwidth featuring up to 80 dB of dynamic range.
- High-speed, low-latency PCI Express x4 (800 MB/s) connection to the host.
- Optimised RF performance with corrections for DC offset, I/Q imbalance and amplitude accuracy.

USRP RIO Block diagram is illustrated in figure 2.7

The following figure shows a simplified block diagram of the USRP-2942 40 MHz. The signal path is duplicated for each of the two channels. The following lists describe the individual blocks: The area within the dotted line indicates the processing on the FPGA when you use NI-USRP with the default FPGA image. When you use LabVIEW FPGA, you control the processing on the FPGA. The RF switch allows transmit and receive operations to occur on the same shared antenna. On the USRP-2942, one antenna is designated receive-only. Receive Path:

- The low-noise amplifier and drive amplifier amplify the incoming signal.
- The phase-locked loop (PLL) controls the voltage-controlled oscillator (VCO) so that the device clocks and local oscillator (LO) can be frequency-locked to a reference signal.

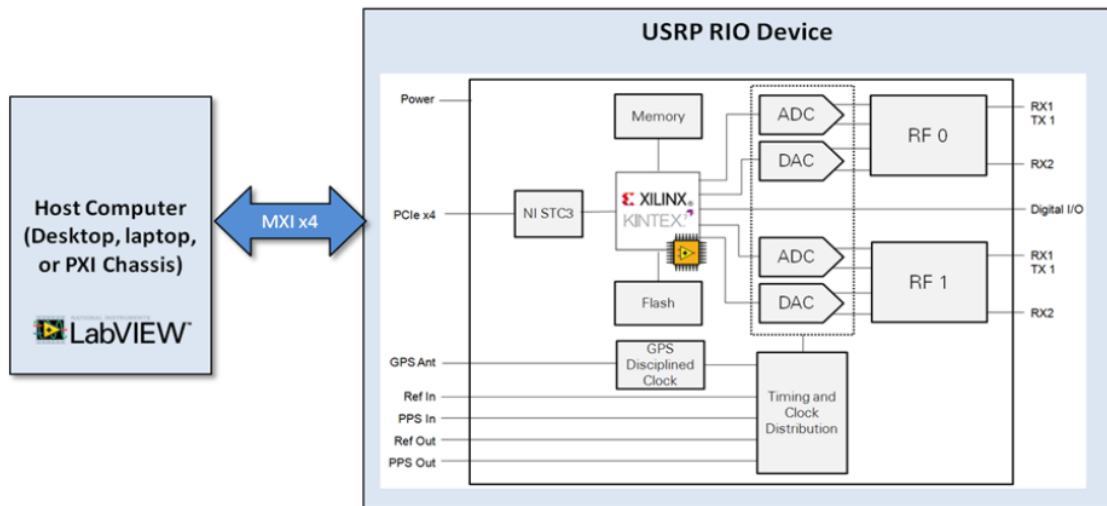


Figure 2.7: USRP RIO Architecture

- The mixer downconverts the signals to the baseband in-phase (I) and quadrature-phase (Q) components.
- The lowpass filter reduces noise and high frequency components in the signal.
- The analog-to-digital converter (ADC) digitizes the I and Q data.
- The digital downconverter (DDC) mixes, filters, and decimates the signal to a user-specified rate.
- The downconverted samples are passed to the host computer over a standard gigabit Ethernet connection. Transmit Path:
 - The host computer synthesizes baseband I/Q signals and transmits the signals to the device over a standard gigabit Ethernet connection.
 - The digital upconverter (DUC) mixes, filters, and interpolates the signal to 400 MS/s.
 - The digital-to-analog converter (DAC) converts the signal to analog.
 - The lowpass filter reduces noise and high frequency components in the signal.
 - The mixer upconverts the signals to a user-specified RF frequency.
 - The PLL controls the VCO so that the device clocks and LO can be frequency-locked to a reference signal.
 - The transmit amplifier amplifies the signal and transmits the signal through the antenna.

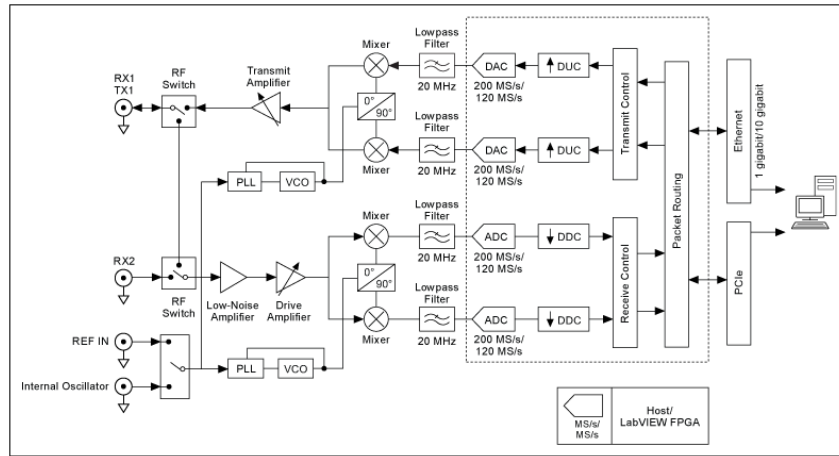


Figure 2.8: RIO datasheet

2.3 LabVIEW Software

NI LabVIEW is a graphical programming platform which is suitable for a variety of control and measurement systems. It offers great integration with existing legacy software and hardware, which makes problem-solving and innovations faster and efficient.

2.3.1 LabVIEW basics

LabVIEW provides the concept of Virtual Instruments (VIs), every program written in LabVIEW appears as a VI, which contains a front panel and a block diagram, as seen in Figure 2.9.

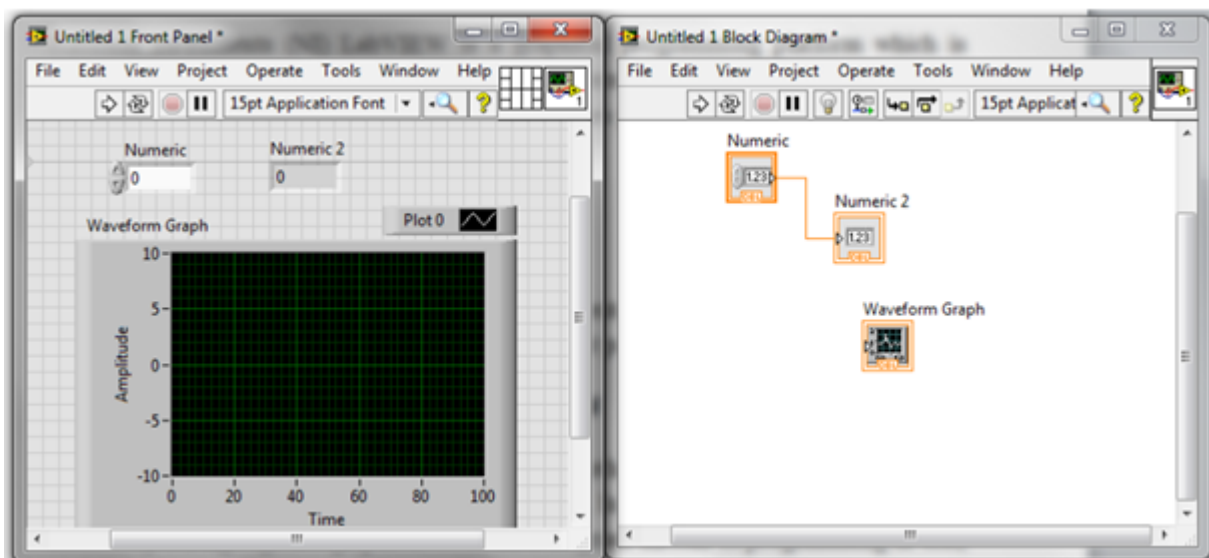


Figure 2.9: Typical LabVIEW VI

The front panel of a VI has the same function as an actual instrument's front panel; designers can add inputs like numeric inputs, switches, connections, etc., as well as indicators

like graphs. The actual programming is done in the block diagram. When creating a user interface component in the front panel, a corresponding icon is also created in the block diagram. The design is done by connecting the icons together to have a block diagram of the specific design. There are also a great number of built-in functions and toolkits, provided by NI, which can be selected for different purposes, and they are very efficient to use while programming [11].

2.3.2 Benefits of programming in LabVIEW

One of LabVIEW's major differences from other general-purpose programming languages is its graphical, dataflow programming style. In LabVIEW, programming is performed by wiring together graphical icons on a diagram instead of programming in text, and those icons are executed according to the rules of data flow. The benefit of the graphical programming is that the users can spend more time on actual system design and focus on problem-solving, rather than spend significant time learning the specific text-based syntax of programming languages. There is a great amount of built-in functions for different purposes provided by National Instruments in different toolkits. The codes generated by the graphical programming language can run as effectively as the traditional C codes.

LabVIEW supports smooth integration with existing software and hardware. LabVIEW contains components like Formula Node, MathScript Node, etc., which provide interfaces for C programming (Formula Node) and Matlab Script (MathScript Node). This expands the range of use of LabVIEW and saves a plenty of time for users, as there is a great number of existing C and Matlab codes for various purposes.

LabVIEW also provides a number of interactive debugging tools such as probes, highlighted execution and dataflow and immediate feedback indicating errors in the code. This makes debugging more easily and also provides monitoring methods while doing measurements and tests [11].

2.3.3 LabVIEW working with NI USRP

According to the advantages mentioned above, LabVIEW is used to control the NI USRP in our implementation. In order to enable LabVIEW to work with NI USRP, a few toolkits and drivers have to be installed, namely NI-USRP 1.2 Driver, LabVIEW Modulation Toolkit, LabVIEW MathScript RT Module, and LabVIEW Digital Filter Design Toolkit.

These toolkits and drivers come with the USRP package and can also be found on National Instruments' websites. And more toolkits and drivers might be needed according to designers' particular requirements [11].

The basic control of NI USRP is very simple through built-in functions as shown in Figure 2.10. It can be divided into three steps [1]:

1. Configure the USRP properties such as sampling rate, carrier frequency, gain, etc.,

according to the designer's needs.

2. Start read (receiver) or write (transmitter) process to receive or transmit data based on the properties selected in first step. This step normally contains loops to receive or transmit continuously.
3. After completing the transmission and/or reception, the USRP connection has to be closed.

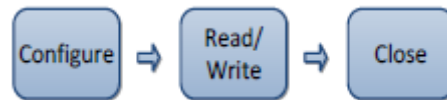


Figure 2.10: Basic steps of controlling USRP via LabVIEW

There are eight built-in functions for USRP control in LabVIEW (NI-USRP driver needed), which are divided into three categories according to the steps mentioned above.



Figure 2.11: The eight most-used NI-USRP functions

The 5 functions in the leftmost column are configure functions used to configure and initiate the USRP as seen in Figure 2.11. The two functions in the middle are used to read/write data from/to the USRP. Finally, the functions in the right most column are used to close the connections between PC and USRP.

Figure 2.12 shows an example front panel of a single channel USRP receiver and Figure 2.13 shows the corresponding block diagram. As shown in Figure 2.12, the user has to select the device names, IQ sampling rate, carrier frequency, active antenna, gain and number of samples before clicking the start button. There are displays for the baseband power spectrum graph and IQ signal graph indicating the current receiving situation. There is also an error output, indicating whether there are errors or not. The selection of sampling rate and number of samples must be within the limitation of USRP and PC in order to avoid errors. The corresponding block diagram shows the actual design of the VI, such as how the components in the front panel are connected and the path and the data flow.

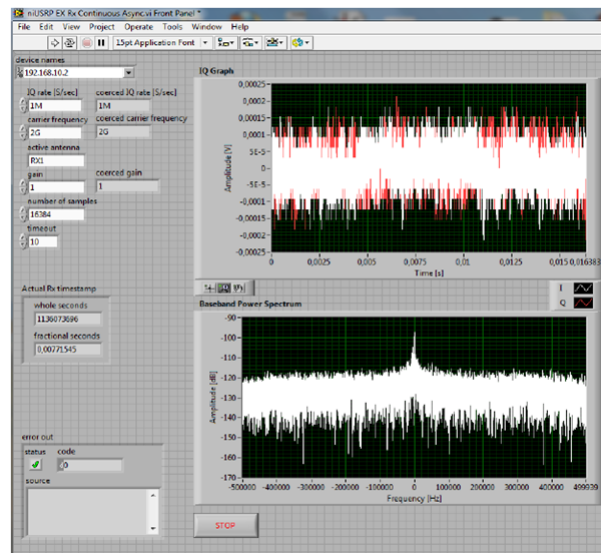


Figure 2.12: Example front panel for USRP receiver

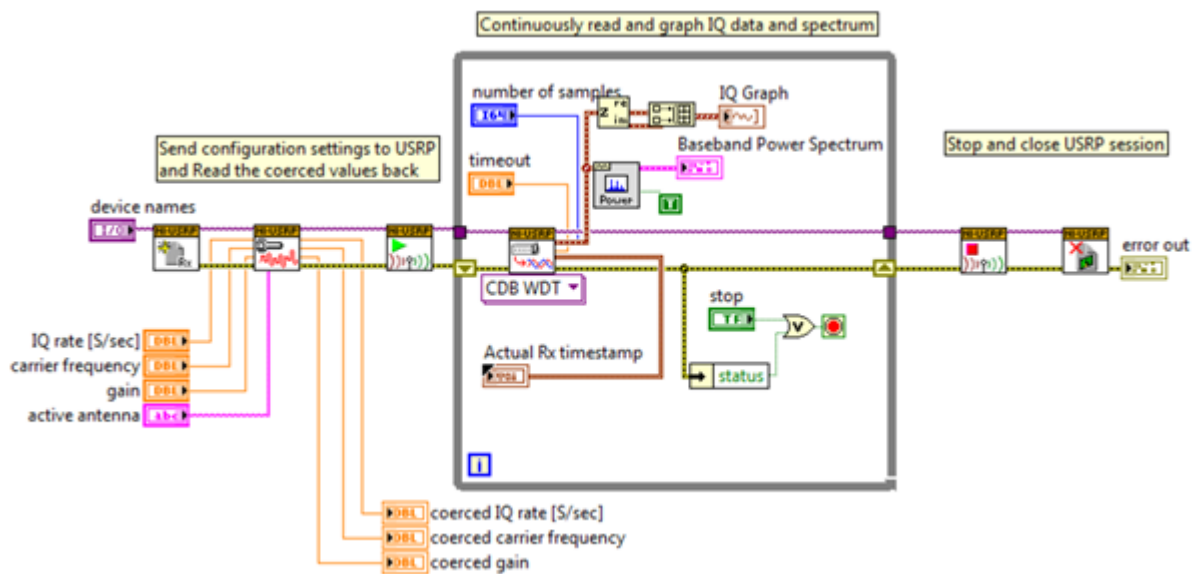


Figure 2.13: Example block diagram for USRP receiver

2.3.4 Description of some modules in LabVIEW

The following section outlines the eight most-used USRP functions. They have been grouped in categories by their functionality, as illustrated in figures 2.10 and 2.11. These categories are: Configure, Read/Write, and Close. These categories are included in most data acquisition programs.

- **Configure Functions**

- **niUSRP Open Rx Session :**

The niUSRP Open Rx Session VI is the first VI that is used to create a software session with the USRP for receiving an RF signal. A session is necessary to send configuration data and retrieve IQ data from the USRP.

- **niUSRP Configure Signal :**

The niUSRP Configure Signal VI can be used with a receive (Rx) or a transmit

(Tx) session. It sets the IQ rate, carrier frequency, gain, and active antenna. For multiple USRP configurations the channel list specifies a specific USRP. Not all IQ rates, frequencies and gains are valid. Always read the coerced values to see if the requested and actual (coerced) values are different.

- **niUSRP Initiate :**

The niUSRP Initiate VI starts the receive session and tells the USRP that all configuration is complete and that the USRP should begin to capture IQ data (samples). This VI can only be used with an Rx session.

- **niUSRP Open Tx Session :**

The niUSRP Open Tx Session VI is the first VI that is used to create a connection to the USRP for transmitting an RF signal. A session is necessary to send configuration data and send IQ data to the USRP. A Tx session can only be used with Tx functions.

- **Read/Write Functions :**

- **niUSRP Fetch Rx Data (Polymorphic):**

The niUSRP Fetch Rx Data VI allows you to retrieve IQ data from a USRP that has an Rx session created with the niUSRP Open Rx Session VI. This data can then be graphed in time domain, or digitally processed for analysis. This VI is polymorphic, meaning that there are several versions (instances) of the VI available to choose from depending on the data type you wish to work with. This VI can only be used with an Rx session.

- **niUSRP Write Tx Data (Polymorphic):**

The niUSRP Write Tx Data VI allows you to send IQ data to the USRP so that it may transmit that data at the carrier frequency specified by the niUSRP Configure Signal VI. This VI is polymorphic, meaning that there are several versions (instances) of the VI available to choose from depending on the data type you wish to work with. This VI can only be used with a Tx session.

- **Close Functions :**

- **niUSRP Abort:**

The niUSRP Abort VI tells the USRP to stop an acquisition in progress. This VI allows you to change configuration settings without completely closing the session and creating a new session. This VI can only be used with an Rx session.

- **niUSRP Close Session :**

The niUSRP Close Session VI closes the current Rx or Tx session and releases the memory in use by that session. After calling this VI you can no longer transmit to or receive data from the USRP until you re-open a new session.

2.3.5 Simulation of BARTLETT & MUSIC Algorithms

- **Simulation of BARTLETT Algorithm:**

As explained in section 1.5.1 , BARTLETT algorithm is a Conventional Beamforming Method, one of the earliest methods of spectral analysis of DOAs. The idea is to guide the antenna beam in one direction (by using weighting vector (w) which acts like a spatial filter) and measure the output power. The directions which result in maximum power yield the DOA estimates.

In this section, we're going to simulate BARTLETT's algorithm in LabVIEW, as shown in figure 2.14. Firstly, A signal is generated with the appropriate angle of arrival then the BARTLETT's algorithm is processed to confirm that the implementation is working well.

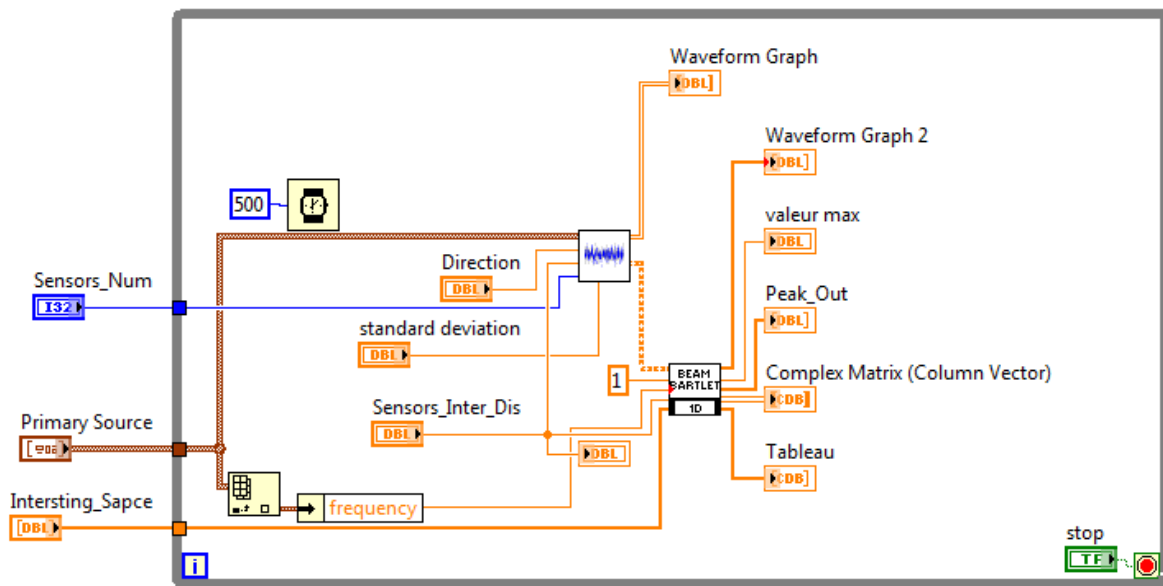


Figure 2.14: Block Diagram of Bartlett's algorithm test

- **Generation module:**

The Module shown in figure 2.15 allows to generate specific signal with the desired parameters .

- **Sine Generation module:**

This module allows to generate sine signal with the desired parameters .

Inputs:

- Sampling rate.
- Frequency.
- Amplitude.

- SNR in order to insert Gaussian white noise.

Outputs:

- Complex BB signal.

Operation: Produce the BB sine waveform with Gaussian white noise where sine's frequency is suitable for given sampling rate. If Nyquist criterion is not fulfilled, then report error.

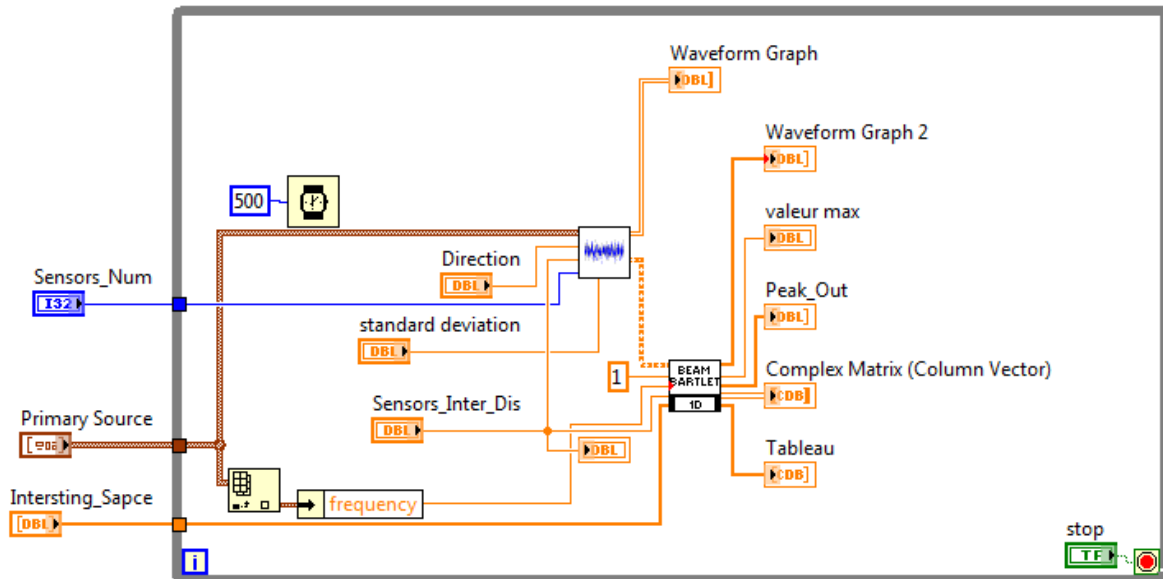


Figure 2.15: Block Diagram of Generation module

- Direction vector : As shown in figure 2.16.
- Input :
- theta Direction of arrival.
- Snapshots.
- Frequency.
- Number of array elements.
- The number of Sensors.
- The number of Sources.
- Wavelength.
- Element spacing.
- SNR.

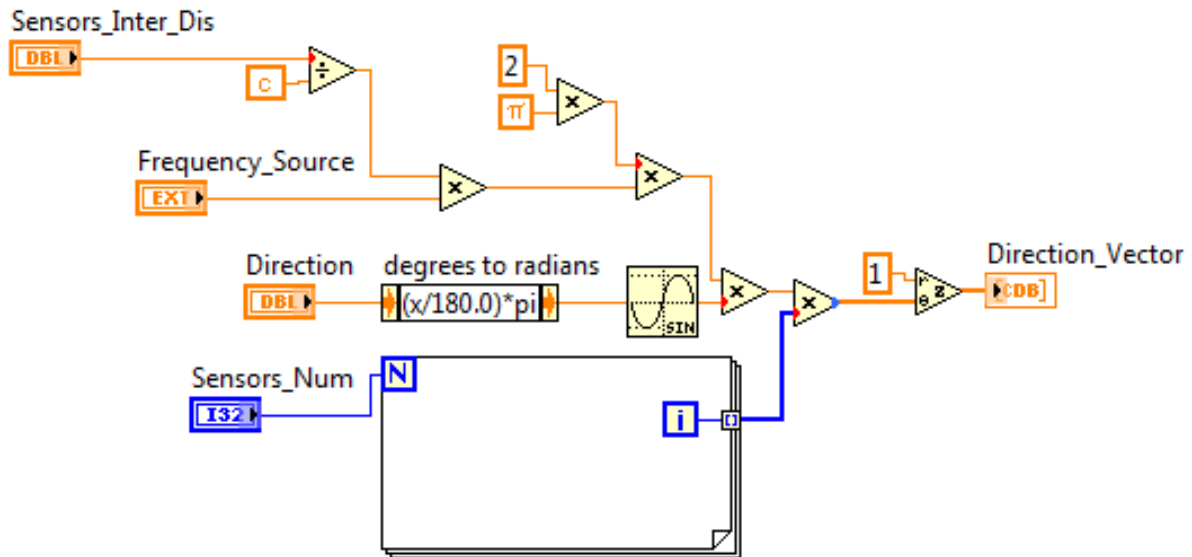


Figure 2.16: Diagram of Direction vector

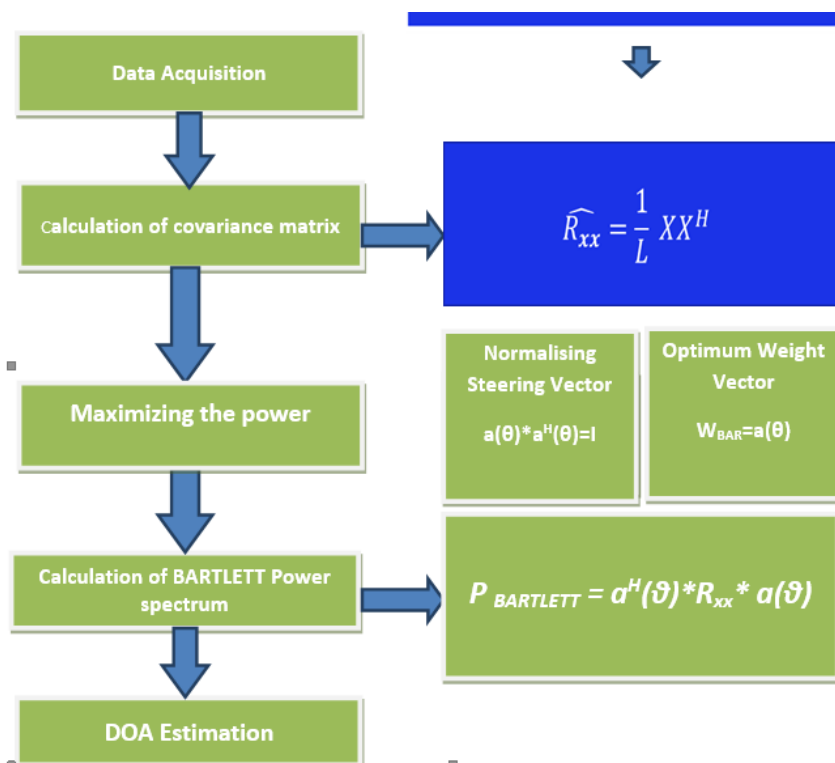


Figure 2.17: BARTLETT Algorithm steps

- **Beam bartlett module:** Figure 2.17 explain the following points:
- Creation of a matrix with P row and M column.
- Calculation of Data covariance matrix.
- Finding the best weights that maximize the power.
- Peak search.
- Display Spatial spectrum function. As can be seen in Figure 2.18.

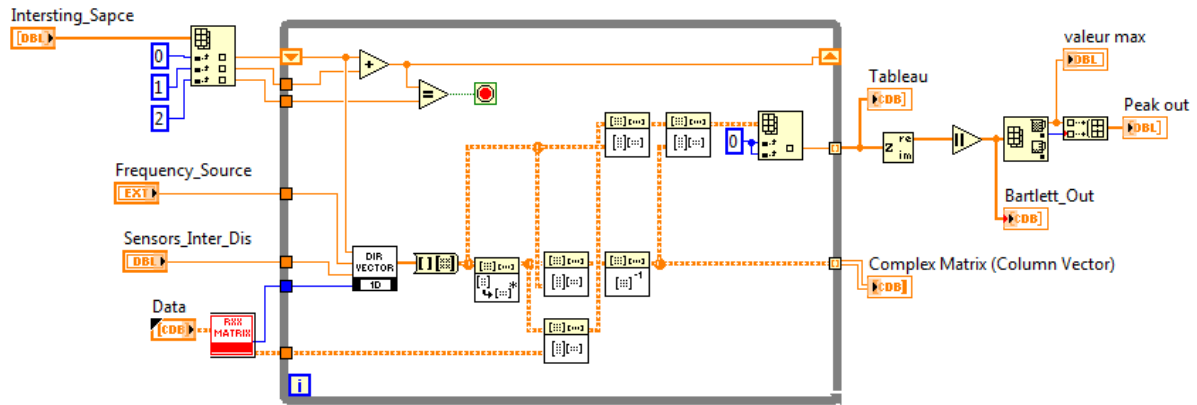


Figure 2.18: Bartlett Beam block diagram

- Display Simulations
- For 2 Sensors and For 10 Sensors:

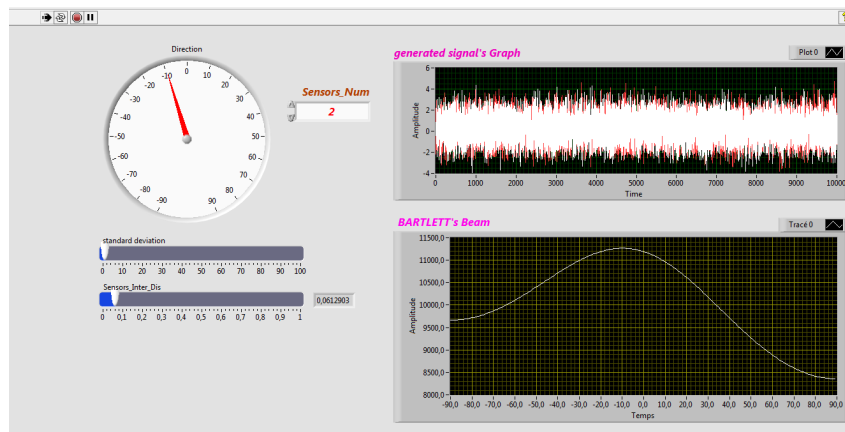


Figure 2.19: Front panel of BARTLETT algorithm with 2 sensors

- **Beam MUSIC module:**
As illustrated in figure 2.21.
- Creation of a matrix with P row and M column.
- Calculation of Data covariance matrix.
- Finding the eigenvalues and eigenvectors of R.
- Estimating noise subspace. As can be seen in figure 2.22.
- Peak search.
- Display Spatial spectrum function. The MUSIC algorithm processing is shown in figure 2.23.
- **Display Simulations**
- **For 2 Sensors and 10 sensors:** The simulation is displayed in figure 2.24 and in figure 2.25.

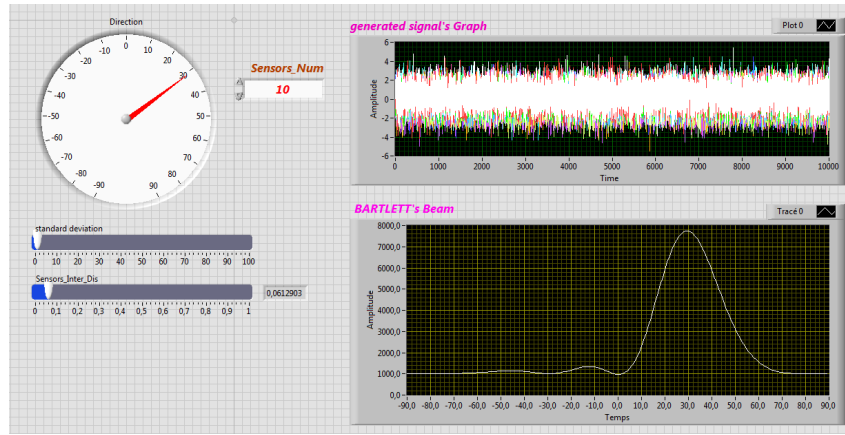


Figure 2.20: Front panel of BARTLETT algorithm with 10 sensors

Figure 2.21: Music Algorithm Steps

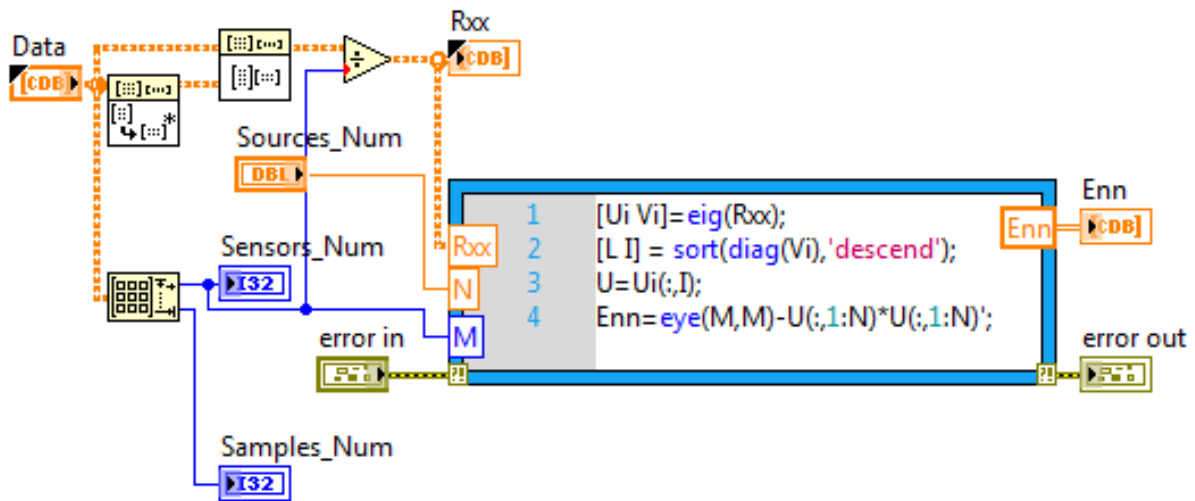


Figure 2.22: Block diagram of Estimating Noise Space

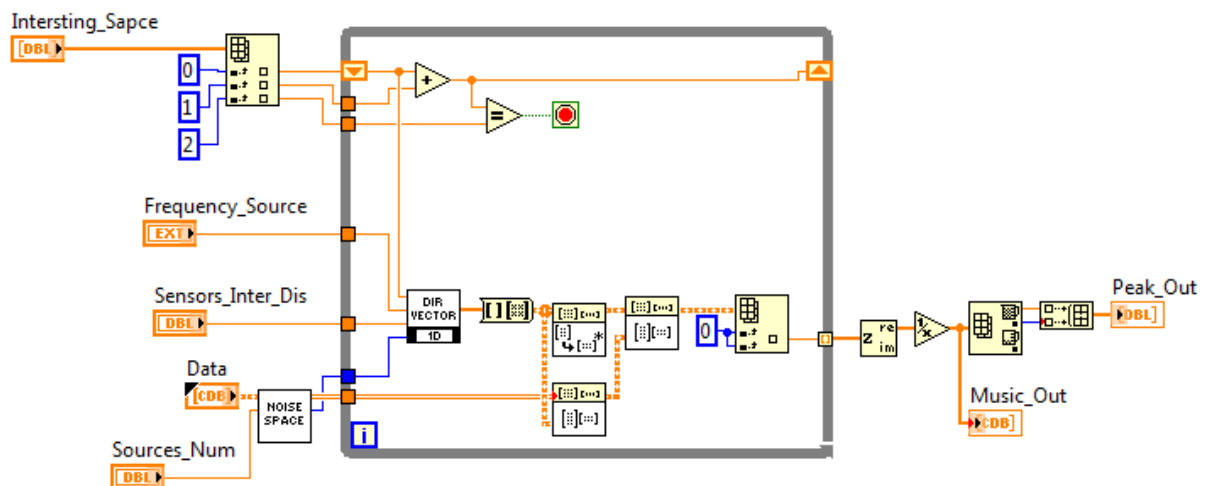


Figure 2.23: Diagram of MUSIC algorithm processing

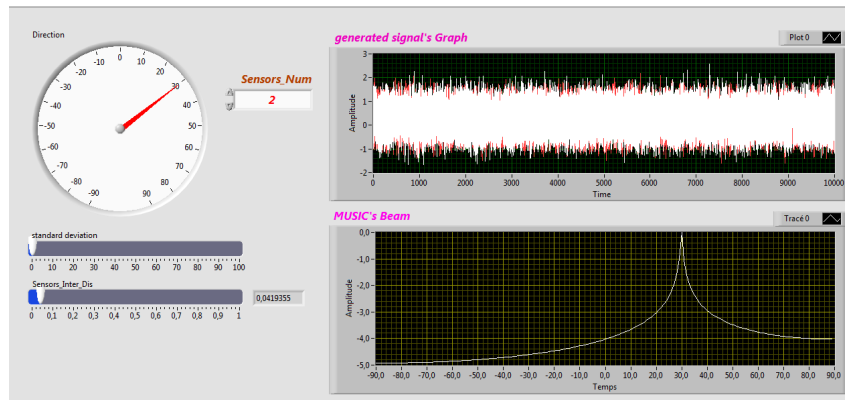


Figure 2.24: Front panel of MuSiC algorithm with 2 sensors

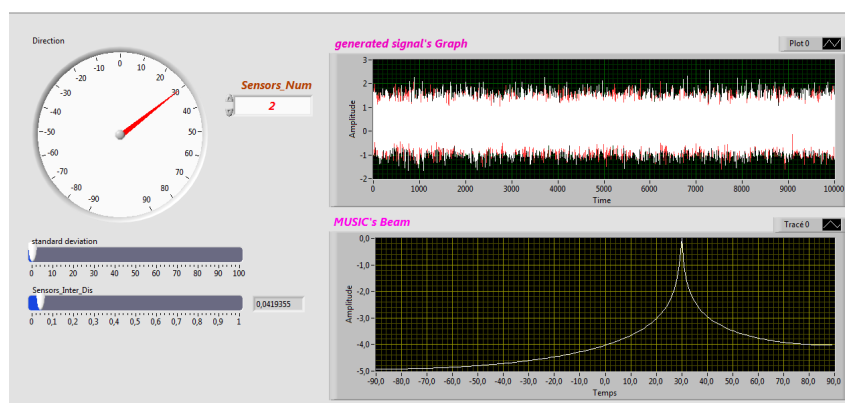


Figure 2.25: Front panel of MUSIC algorithm with 10 sensors

Chapter 3

Setup of localization system

3.1 Transmitter and receivers

TX data can be analog (sound) or digital signal (bits) which we want to transmit.

TX Base-Band (BB) processor gets TX data signal and produce BB complex signal which is suitable to channel and RF equipment requirements (bandwidth, transmission rate). This unit can be implemented in software (MATLAB, NI-Labview, C) or in hardware (DSP or ASIC).

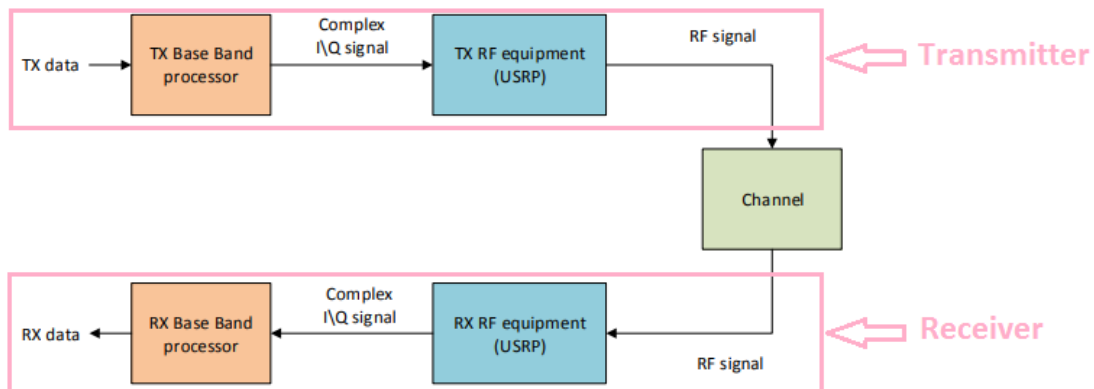


Figure 3.1: Generic communication system

- TX data can be analog (sound) or digital signal (bits) which we want to transmit.
- TX Base-Band (BB) processor gets TX data signal and produce BB complex signal which is suitable to channel and RF equipment requirements (bandwidth, transmission rate). This unit can be implemented in software (MATLAB, NI-Labview, C) or in hardware (DSP or ASIC).

- TX RF equipment obtains BB digitally represented signal, converts it to analog signal by Digital to Analog converter (DAC). Analog signal is up-converted to RF frequencies and transmitted through antenna to the channel. In our project TX RF equipment is easily implemented by configurable NI –USRP modules.
- Channel can be represented by cable or wireless medium. Channel may introduce impairments, like attenuation, distortions, fading of the signal.
- RX RF equipment performs opposite operation to the TX RF transmitter. This unit down converts the received signal to the BB and using Analogue to Digital Converter (ADC) converts it to the digital representation of the received signal.
- RX Base-Band processes the BB received signal in order to detect the transmitted data.

3.1.1 Transmitter

The USRP receives a waveform from the host PC with 16 bits of resolution sampled at up to 25 MSamples/second. This signal is up-converted to a radio frequency (RF) before being sent to an amplifier and then transmitted over the air.

- The graphical interface (GUI) for USRP module, which working in the TX mode

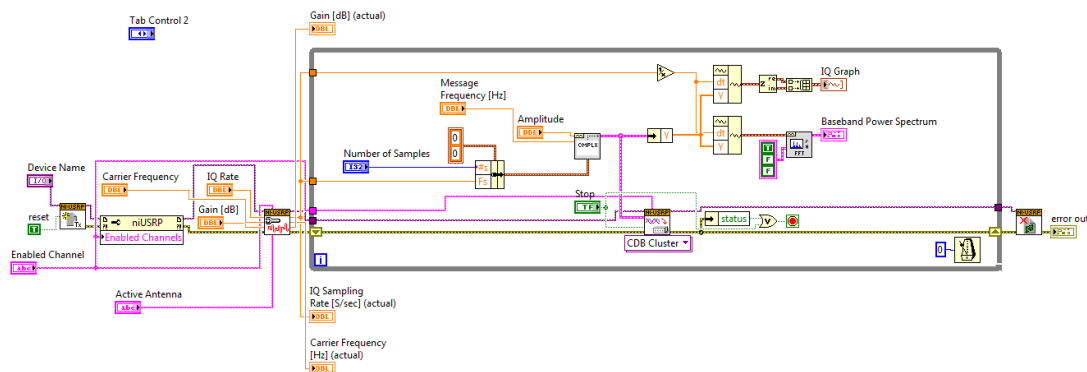


Figure 3.2: Block diagram of Sinus transmitter

- Sine Generation module:

Inputs:

Sampling rate Frequency Amplitude

Outputs:

Complex BB signal

Operation:

Produce the BB sine waveform Verify that sine's frequency is suitable for given sampling rate. If Nyquist criterion is not fulfilled, then report error.

The front panel of the IQ graph is:

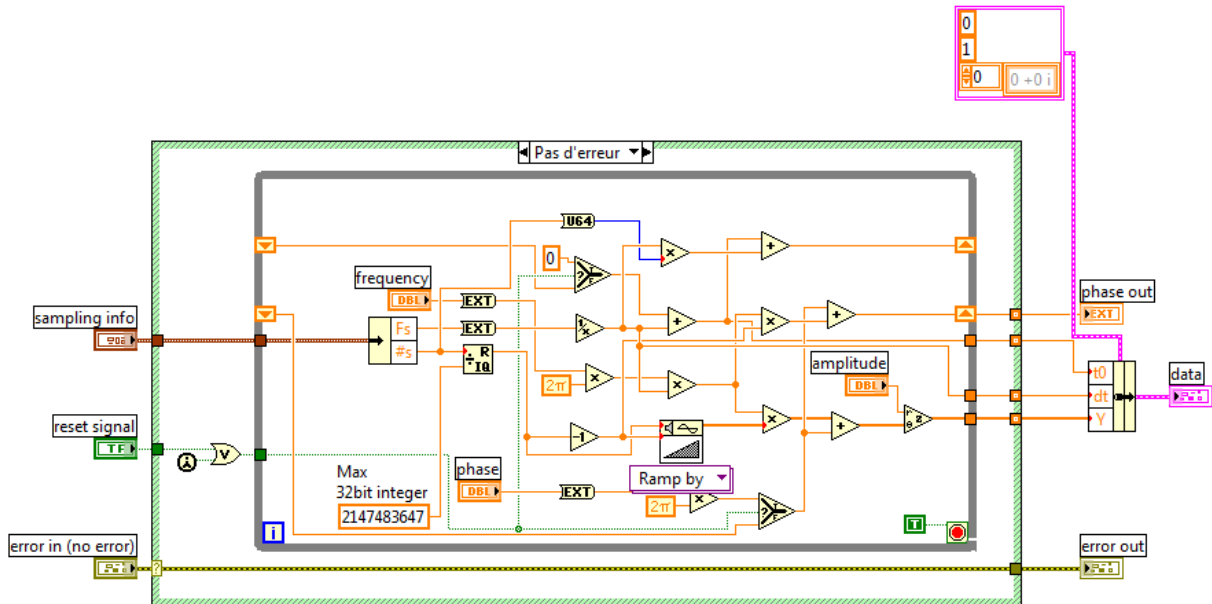


Figure 3.3: Block diagram of Sine Generation module

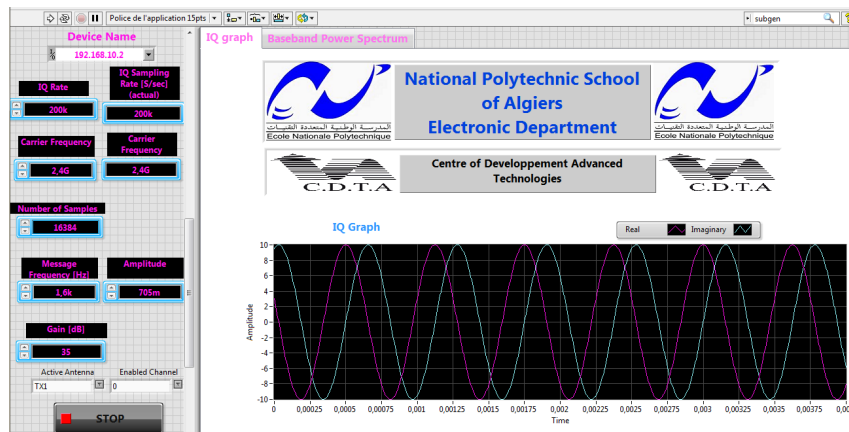


Figure 3.4: TX front panel tool

As we can see on the Figure 3.4 we define all USRP configurations: sampling rate, carrier frequency, IP address of the USRP card and we set the reference frequency and finally we can start the transmission by click on the 'play' button.

The Baseband spectrum of the transmitted signal is shown in figure 3.5

3.1.2 Receiver

The received RF signal is down-converted to a complex I/Q baseband signal sampled at 1 MSamples/second. The digital signal is then down sampled to a rate specified by the user and passed to the host PC for processing. When the ADC of the NI USRP samples at the full digitizer rate (1 MSamp/sec), it can acquire a bandwidth of 20 MHz. Sampling at

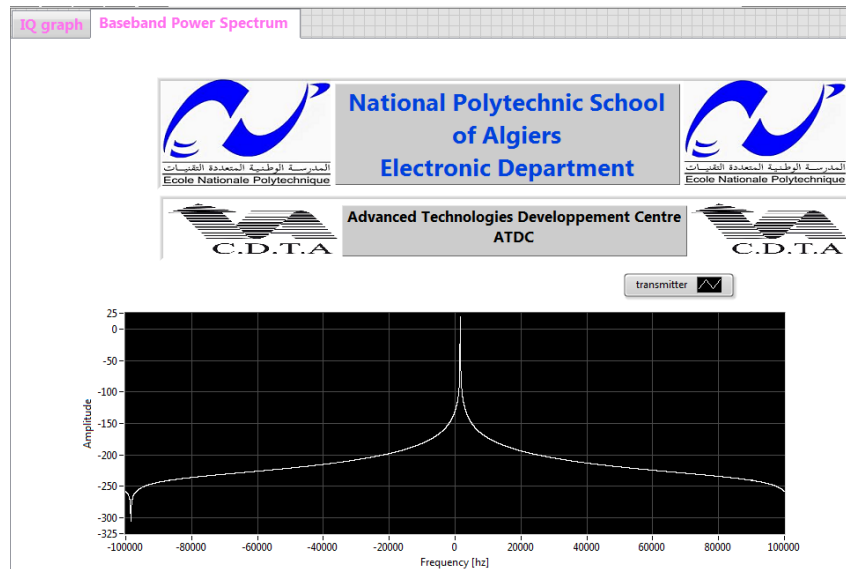


Figure 3.5: Baseband power spectrum of the transmitted signal

such high rate with high resolution (14 bits) produces a large amount of data. However, to acquire a signal with smaller bandwidth (a narrowband signal), it is sufficient to sample at a rate at least two times larger than the signal bandwidth (according to Nyquist sampling theorem).

- This section introduces the graphical interface (GUI) for USRP module, which working in the RX mode.

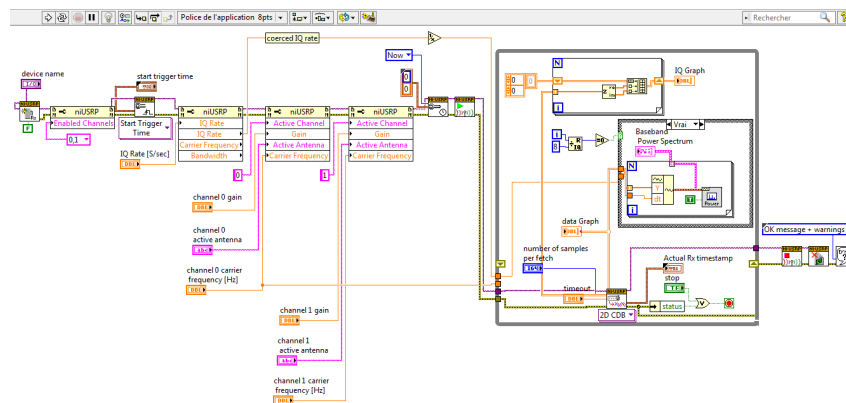


Figure 3.6: Block diagram of a receiver with USRP RIO card

The front panel of the received signal is given in Figure 3.7

3.2 Multi devices synchronization

3.2.1 signals of common reference

NI USRP devices take two reference signals for time and frequency synchronization:

- One pulse per second (PPS IN) to synchronize the sampling time between the de-

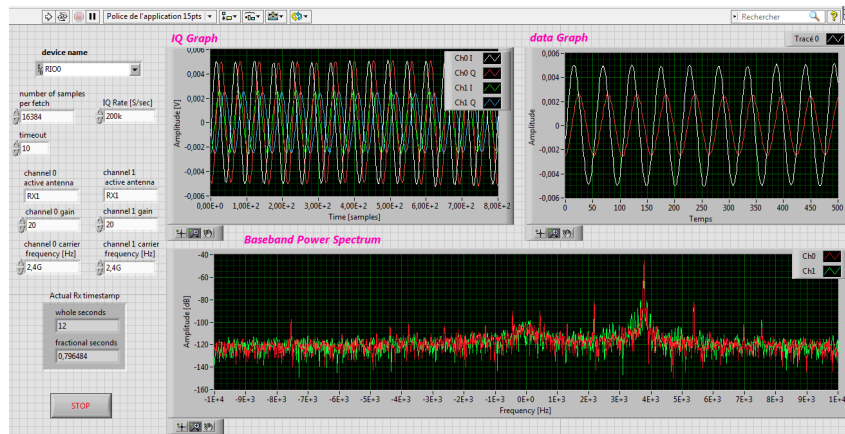


Figure 3.7: Front panel of RX tool

VICES: it is a square shaped electrical signal (slots) transmitting a time information (number of pulses per second) by a SMA connector, Synchronization is performed on the rising edge of the pulse.

For the rest, the PPS is not normalized, that is to say each user can define the amplitude of the slots (the level 5 V is current) or the duty cycle of the square signal. The output impedance is often 50 Ω in order to be adapted to that of the coaxial cables.

- A 10 MHz frequency reference (REF IN): This is an external reference signal for the local oscillator (LO) on the device. It is an SMA connector with an impedance of 50 Ω and a minimum input power of 0 dBm and a maximum of 15 dBm for a square or sinusoidal wave to provide a unique frequency reference for both devices.

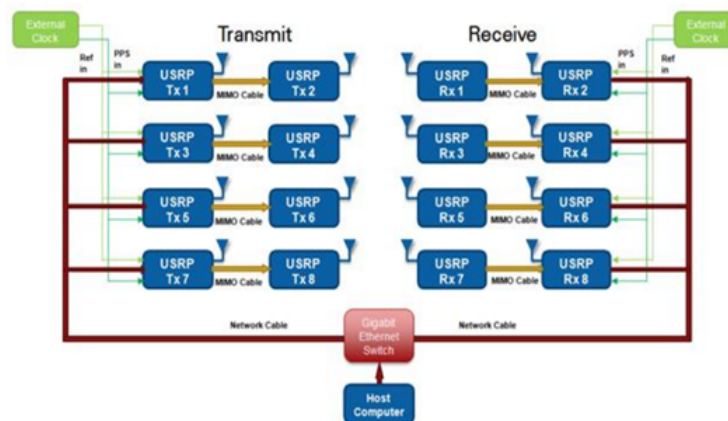


Figure 3.8: Synchronization of multiple USRPs

3.2.2 synchronization of two USRPs with MIMO cable

Some applications require synchronization across multiple USRP (Universal Software Radio Peripheral) devices. For example, two USRPs can be synchronized using a MIMO cable.

- MIMO system requirements are Time and Frequency synchronization , For a transceiver to be considered MIMO-capable, each channel in the system must meet two basic requirements:
 1. The sample clocks must be synchronized and aligned.
 2. DSP operations must be performed on samples aligned in time – from the same sample clock edge.

- A MIMO cable: transmitting a coded time message from one device to another and assure the synchronization.

This method does not require a separate PPS and REF input to the devices, but it is limited to a total of 2 USRPs.

A USRP2 device can synchronize its time to another USRP device via the MIMO cable. Unlike the other methods, this does not use a real "pulse per second". Rather, the USRP device sends an encoded time message over the MIMO cable. The slave device will automatically synchronize to the time on the master device.

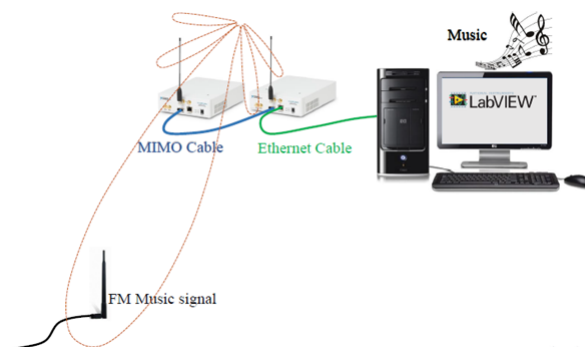


Figure 3.9: USRPs receivers with MIMO cable

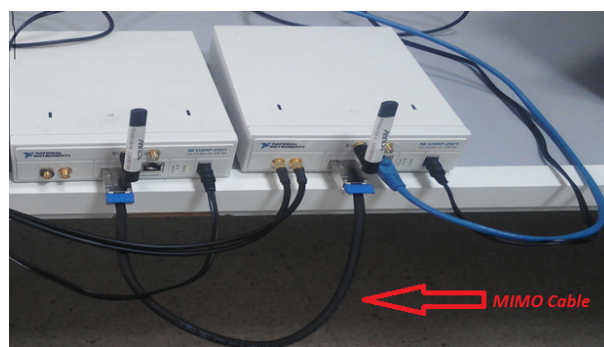


Figure 3.10: Synchronization of two USRPs with MIMO cable

- The MIMO cable allows two USRP devices to share reference clocks, time synchronization, and the Ethernet interface. One of the devices will sync its clock and time references to the MIMO cable. This device will be referred to as the slave, and the other device, the master.

- The slave device acquires the clock and time references from the master device.
- The master and slave may be used individually or in a multi-device configuration.
- External clocking is optional and should only be supplied to the master device.

Shared Ethernet mode

In shared Ethernet mode, only one device in the configuration can be attached to the Ethernet.

- Clock reference, time reference, and data are communicated over the MIMO cable.
- Master and slave must have different IPv4 addresses in the same subnet.

Dual Ethernet mode

In dual Ethernet mode, both devices in the configuration must be attached to the Ethernet.

- Only clock reference and time reference are communicated over the MIMO cable.
- The master and slave must have different IPv4 addresses in different subnets.

3.3 USRP RIO's channels synchronization

Some applications, such as beamforming and direction finding, place additional requirements on the system. In addition to sample time and sample clock alignment, the system must maintain a known phase relationship between each RF input or output. In order to achieve phase alignment between the USRP RIO Channels, Both of the channels must be aligned with each other (in the same starting point). This is achieved by using flow commands (TRIGGER), which tells the USRP to start at a specified time. Since the devices are synchronized via the MIMO cable, the USRP starts at exactly the same time (transmission or reception). Due to phase ambiguities caused by phased-locked loops (PLL) which are used for up and down-conversion, some calibration may be required to determine this phase relationship. a phase shift may occur between the Channels of USRP RIO (before sampling), which is usually deleted by the user, using a training sequence to estimate the offset. This is necessary after each initialization: This phase shift depends on the LO frequency. Other components outside the local oscillator contribute to phase shift (Filters, Mixers, amplifiers, and other components produce phase shifts that vary with time and temperature). This phase shift (which is random) remains constant after the reset until the device is closed or readjusted. Periodic calibration will therefore be necessary for coherent phase applications. At this point, the phase difference between the

received signals is caused by the initial phase differences of the LOs . The front panel of the phase calibration program developed in LabVIEW for phase calibration is shown in Figure 3.12. The figure shows the initial phase differences between the signal received from the reference antenna and the other three antennas. Once the phase differences are measured, phase offsets are introduced in the received signals to compensate for these phase differences. Figure 9 shows the calibrated signals after introducing phase offset. It is possible to calibrate a multi-channel system by producing a tone that is distributed to each input of the device. To do that, We opted for two methods . An illustration of a system that uses this methodology is shown in this part. However, we developed two softwares running on the host PC to measure the phase difference of each channel and apply a correction. We used identical cables with a splitter to connect each channel of the receiver to the transmitter as shown in the following figure 3.11.

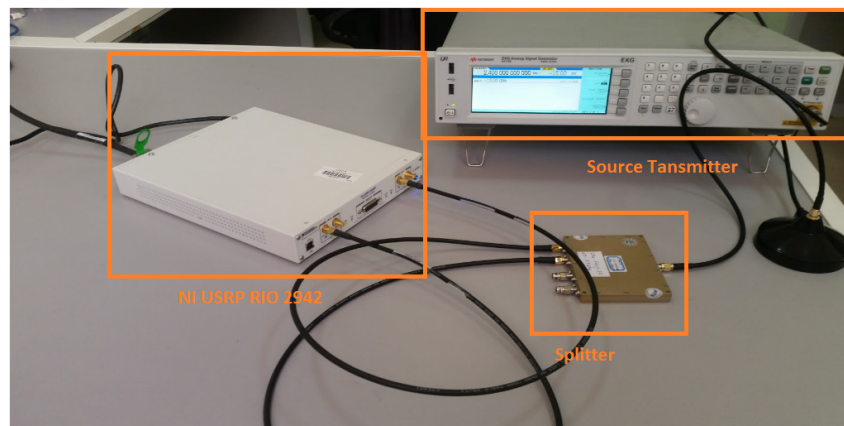


Figure 3.11: multi-channel system calibration

- **Source transmitter** : is an electronic device that generates repeating electronic signals in either the analog or the digital domain, Used in our case for testing .
- **Splitter** : Power dividers (also power splitters) and directional couplers are passive devices used mostly in the field of radio technology. They couple a defined amount of the electromagnetic power in a transmission line to a multi port enabling the signal to be used in another circuit.
- **NI USRP RIO 2942** : The two channels of the RIO card are used as a receiver.

3.3.1 Phase calibration using LabVIEW module

At this point, the phase difference between the received signals is caused by the initial phase differences of the LOs .

The front panel of the phase calibration program developed in LabVIEW for phase calibration is shown in Figure 3.12.

The figure shows the initial phase differences between the signal received from the reference antenna and the other three antennas.

Once the phase differences are measured, phase offsets are introduced in the received signals to compensate for these phase differences.

Figure 3.13 shows the calibrated signals after introducing phase offset.

The RF receivers used in the system are independent, which means that each RF receiver has its own local oscillator (LO).

The LOs are connected to the same clock signal generated by the NI USRP RIO board.

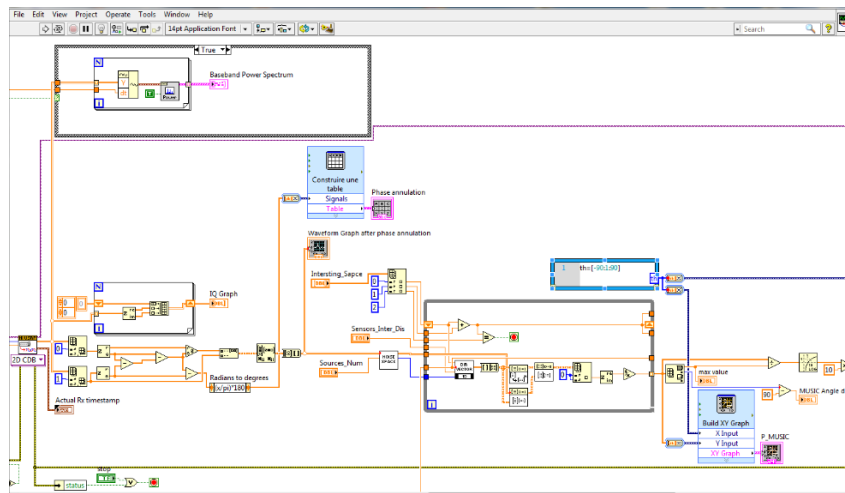


Figure 3.12: phase compensation bloc diagram

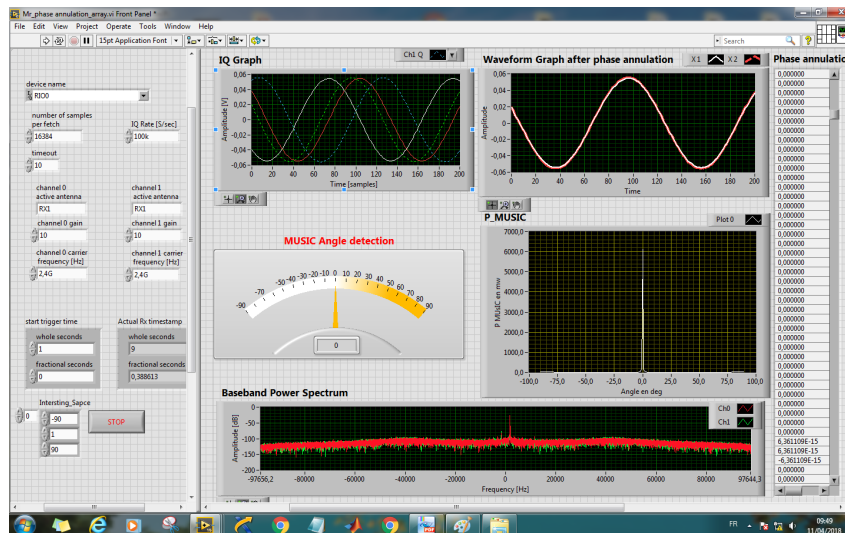


Figure 3.13: Phase shift before and after phase calibration Front Panel

3.3.2 Phase calibration using correlation

To calculate phase shift with correlation we used three methods:

1. Using MATLAB Script:

2. Using FFT:

3. Using LabVIEW module:

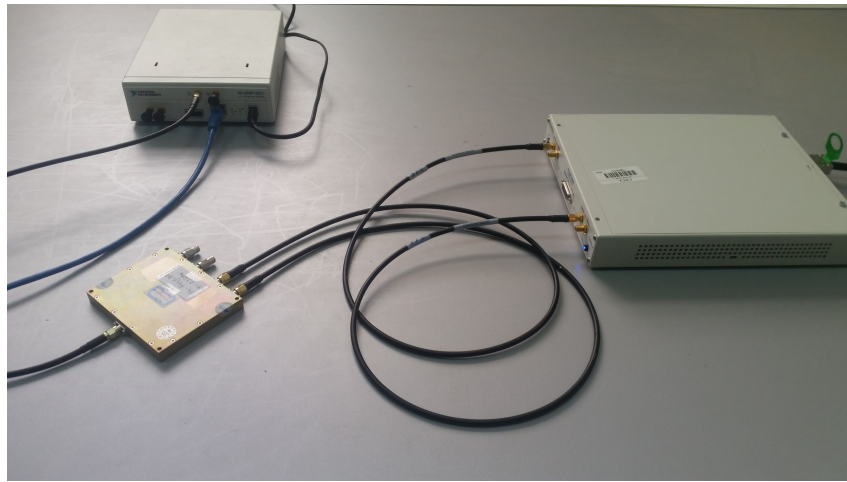


Figure 3.14: Multi channel cabled system for Correlation method phase detection

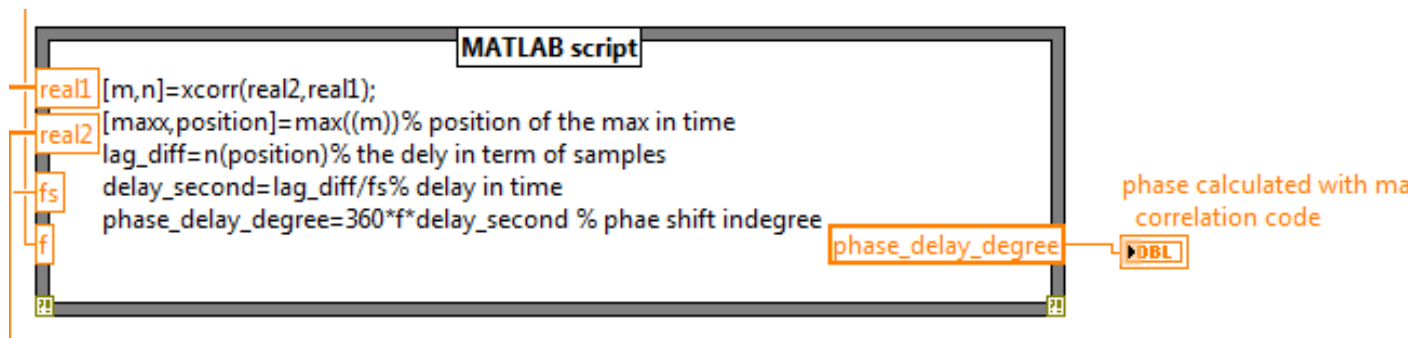


Figure 3.15: Phase shift using MATLAB script

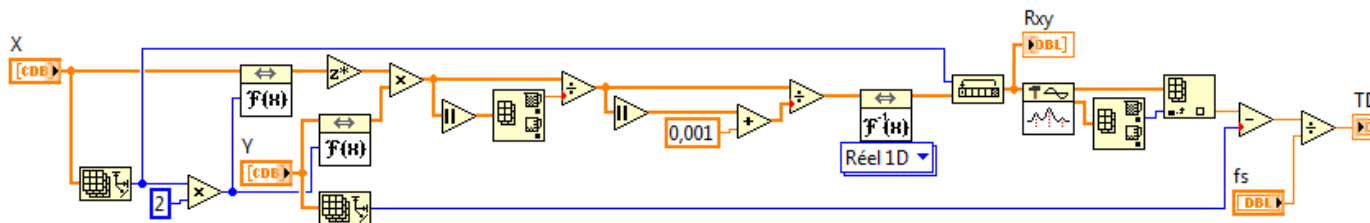


Figure 3.16: Phase shift using FFT method

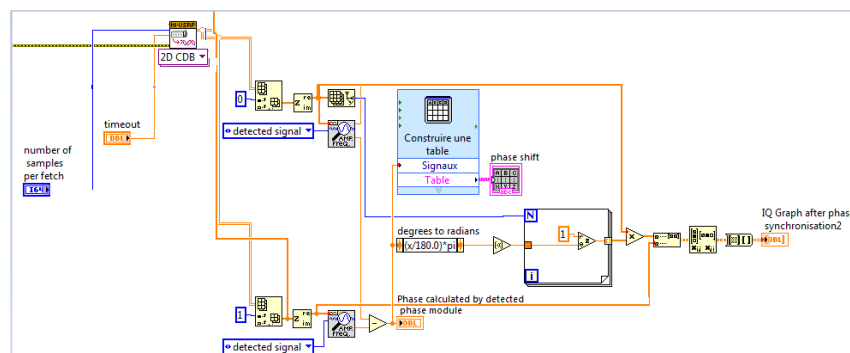


Figure 3.17: Phase shift using LabVIEW module

3.4 MUSIC & BARTLETT Algorithms implementation

This part covers the details of implementation for testing the Music and Bartlett algorithms used for this project. The system contains two parts as transmitter and receiver. As

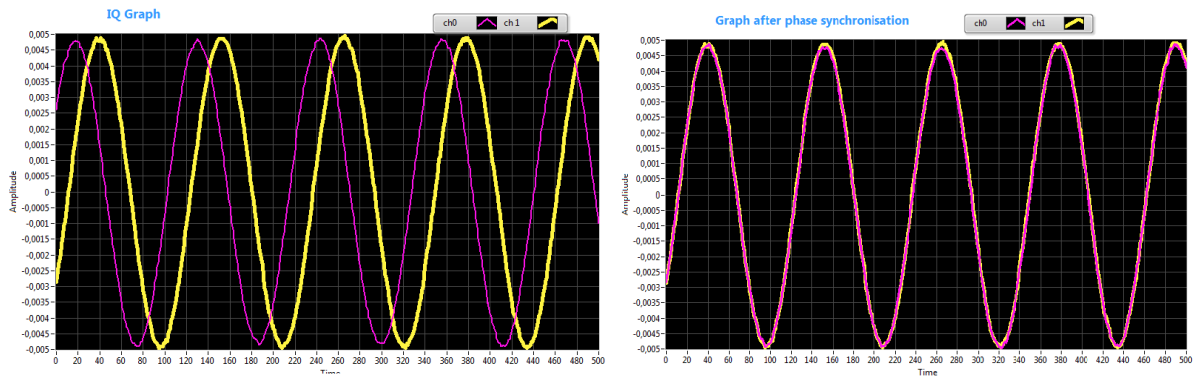


Figure 3.18: Received graph before synchro- Figure 3.19: Graph of the signal after phase synchronization

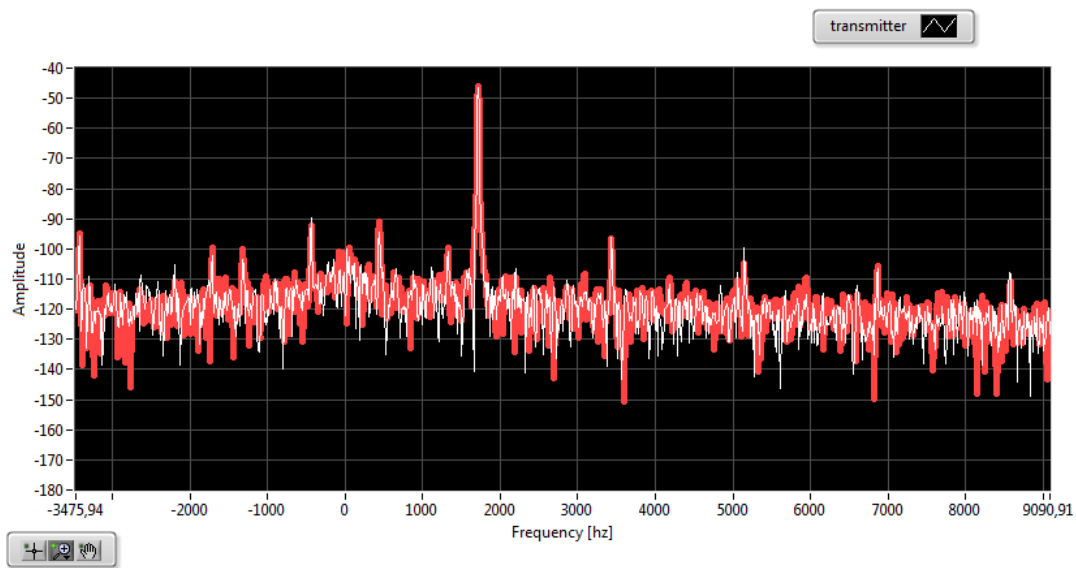


Figure 3.20: Baseband Power spectrum of the received graph

shown in Figure ??, the transmitter is implemented using NI USRP-2921 with LabVIEW controlled by PC using in order to control the frequencies, gain and more parameters. The receiver is implemented using NI USRP-2942 and PC with LabVIEW and specific toolkits.

The RF Direction of Arrival (DoA) detection system has been implemented with NI USRP RIO hardware in LabVIEW 2015. The material below is relevant to LabVIEW version. We describe how to implement the RF Angle of Arrival (AoA) detection system with NI USRP RIO 2942 hardware and NI USRP 2921 hardware. This system uses two methods for correcting USRP phase ambiguities, so there is a cabled system.

Hardware Configuration:

The following hardware was used to implement this system:

One PC with a free Gigabit Ethernet port

USRP Ts (NI USRP 2921 were used)

USRP RIO RXs(an NI USRP 2442R was used)

3 antennas

BNC splitter T's cables, and SMA to BNC adapters.

External signal Generator.

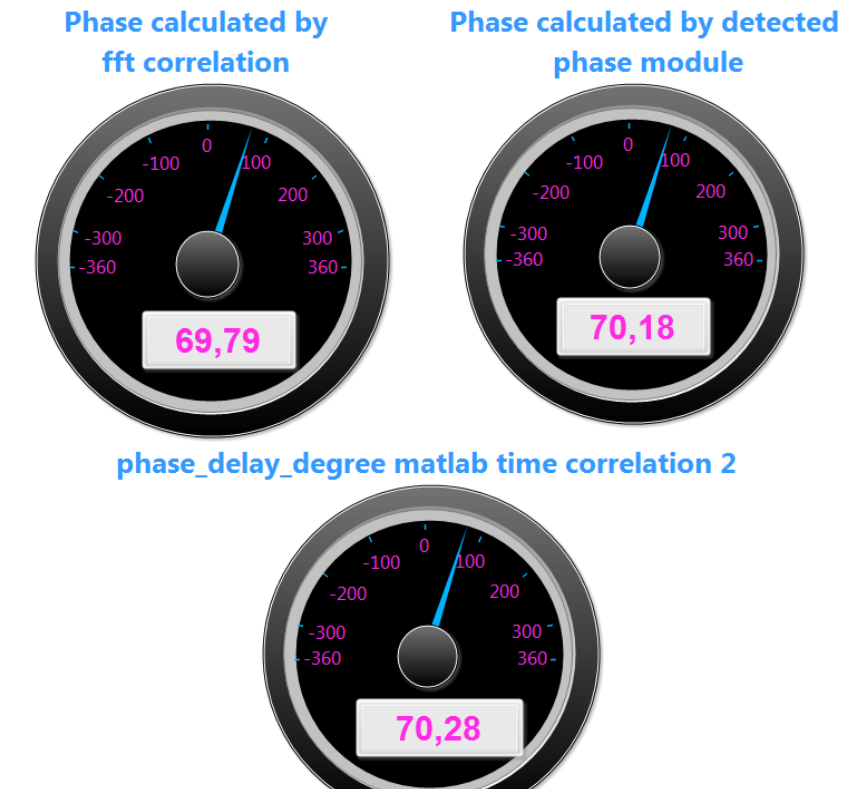


Figure 3.21: The three phase shift detected

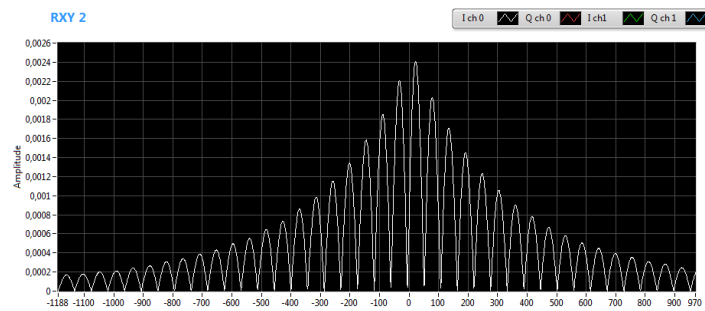


Figure 3.22: Cross correlation graph of the two components of the received signal

- We have also connected one antenna to each of the four USRP RX ports on the USRP RIO devices that are going to serve as the receiver (NI recommends using RX1/TX1 port for simplicity).
- We have also connected one antenna to each of the four USRP RX ports on the USRP RIO devices that are going to serve as the receiver (NI recommends using RX1/TX1 port for simplicity).
Both receiving antennas should be exactly half a wavelength (of the carrier frequency used) apart.

Calculating the distance between antennas :

$$\lambda = \frac{c}{f_c}$$

$$\lambda = \frac{3 * 10^8}{2.4 * 10^9} = 0.125m$$

$$d = \frac{\lambda}{2} = 6.25cm$$

- The USRP 2921 is connected with appropriate gigabit Ethernet cable.
- A Gigabit Ethernet cable is connected to the host PC.
- The USRP RIO is connected to the host PC via PCIe x4.

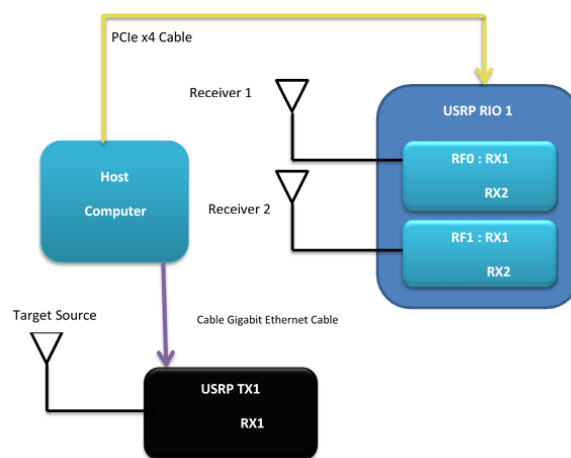


Figure 3.23: The DoA Detection System with USRP RIO and USRP Hardware Setup Diagram

3.4.1 Hardware Setup

The experimental setup components are composed of :

- USRP 2921 and USRP RIO R2942 boards
- 3 antennas where two receivers antennas and a transmitting antenna as a target source and a computer.
- The Omni directional antennas are attached to the USRP Rio 2942 board in order to implement a uniform linear array of 2 elements which are half-wavelength spaced. Each antenna is connected to a channel board via SMA connector.

This board is connected to the computer via PCIe cable. The third antenna is connected to a channel board via SMA connector of USRP 2921 board.

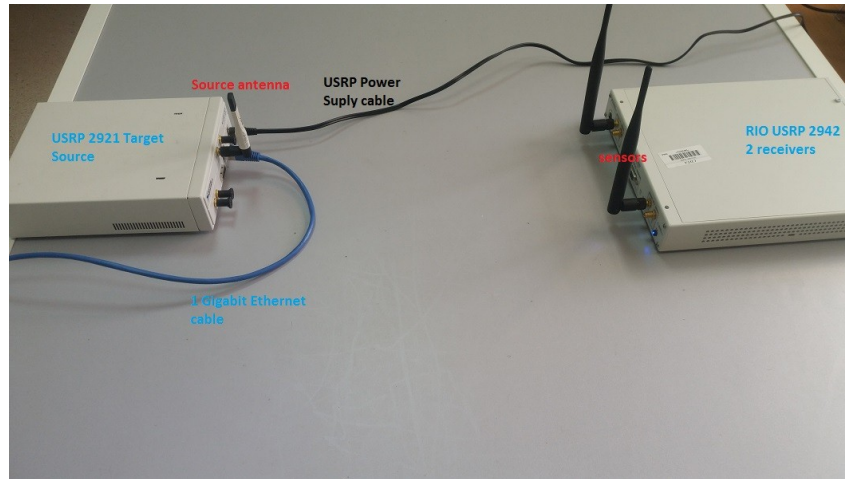


Figure 3.24: The AoA Detection System with USRP RIO and USRP Hardware Setup Diagram

3.4.2 Software Configuration

- Target Source transmitter:

The front panel of our target source transmitter contain the parameters for the NI USRP transceivers that are used for transmitting signals.

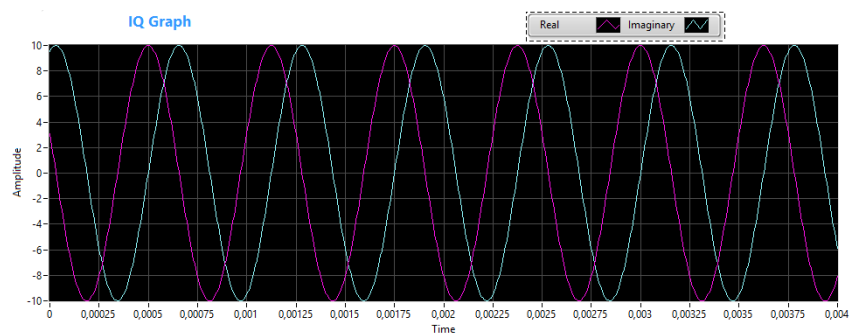


Figure 3.25: Target Source transmitter IQ graph front panel

It is clear that the the IQ graph seen if figure 3.25 is a complex signal with sinusoidal components. We have set the controls of these parameters as follows: Device Names :

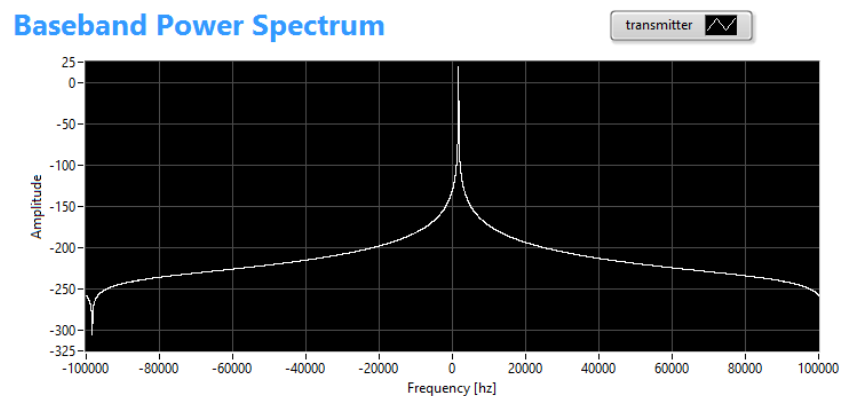


Figure 3.26: Target Source transmitter baseband power spectrum graph front panel

We enter the IP addresses associated with the USRP TX1. Active Antennas : We enter the appropriate antenna ports TX1 that we connected the Target Source antenna to NI USRP 2921. I/Q rate [S/sec], and carrier frequency [Hz] : For the I/Q rate, and carrier frequency we enter the sample rate, and the carrier frequency. These parameter values have to be the same for both the transmitter and receiver. timeout: timeout specifies the time to wait in seconds, before returning an error if the requested number of samples have not been generated. A negative value indicates to the driver to wait indefinitely. tone frequency: tone frequency specifies the frequency of the transmitted signals. In our case we have chosen 1.6 KHz for our target source. Amplitude : specifies the amplitude of our target source signal. We select 0.705 V. Gain : Enter the appropriate gain values for all the USRP 2921.

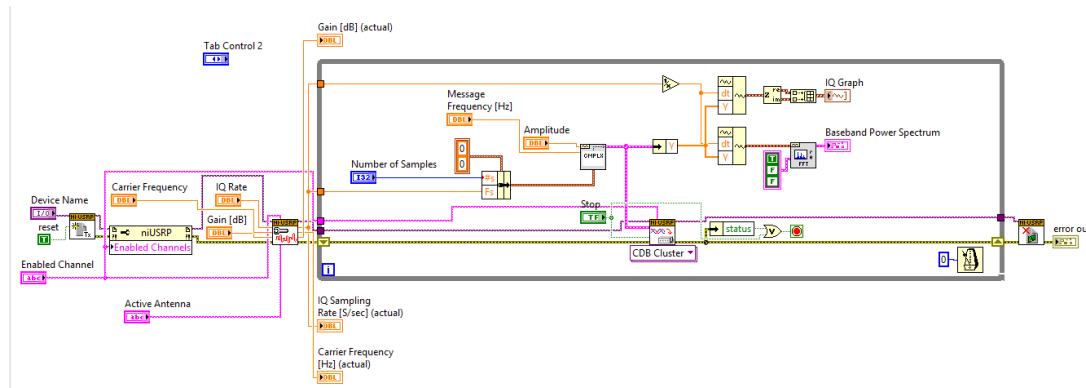


Figure 3.27: Target Source Transmitter Block Diagram

Figure 3.27 presents the block diagram of the Target Source Transmitter Block Diagram. As can be seen from the block diagram, it opens the target USRP TX session. Then it starts to continuously transmit a sinusoidal tone of given parameters. This signal is considered as the target signal whose AoA at the receiver is to be detected.

- Receiver :

The receiver part is implemented with NI RIO USRP-2942 connected to a PC with LabVIEW via PCIe x4 cable. The programming and design are realized in LabVIEW in order to control the USRP hardware. As introduced in Chapter 2, a LabVIEW program or VI contain two parts, the front panel and the block diagram. The front panel is the user interface, like the front panel of a real instrument, and the block diagram is the actual programming part. The details of the implementation are given in this section.

Figure 3.28 presents the block diagram of AoA Detection RX Localization using MUSIC. The RX VI sets up the USRP Rio at Both of the receiving channels to have the appropriate operating configurations. It first captures a specified number of samples per processing cycle. The phase calibration to eliminate the uncertainties is done based on the information provided by the calibration signal. After the target signal is calibrated, it is then fed to the MUSIC algorithm to detect the AoA. Receiver VI Front Panel The front panel of the receiver VI is divided into two parts. The left half is represented in Figure 3.29 and represents the configuration part, and the right part is used for monitoring the test states and displaying the test results.

The left part of the front panel contains two main parts, the configuration of USRP hardware settings and the configuration of parameters for AoA Music algorithm. As seen in Figure 3.29, the USRP hardware configuration block contains the settings such

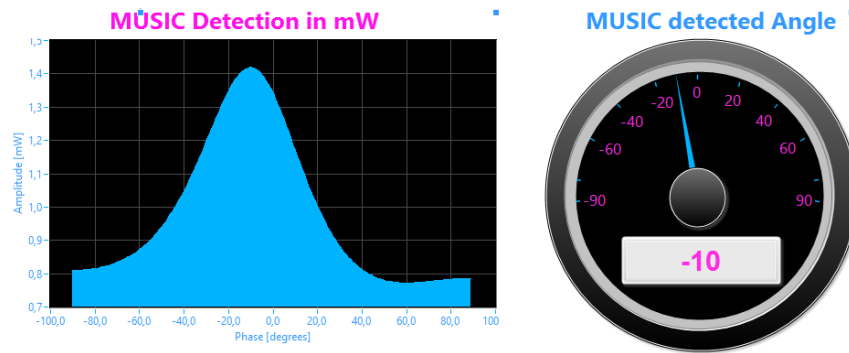


Figure 3.28: Receiver VI front panel

as device name, IQ sampling rate, carrier frequency, RX antenna selection and gain, and number of samples per fetch.

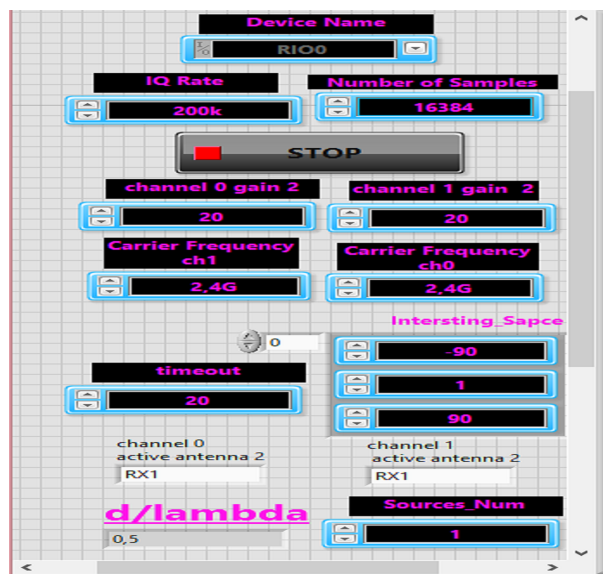


Figure 3.29: USRP hardware configuration block

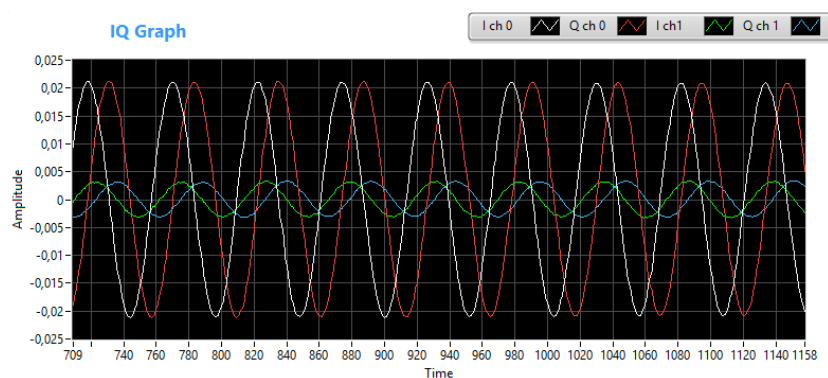


Figure 3.30: receiver IQ graph front panel

As seen in Figure 3.30 the right half of the VI's front panel is used for monitoring and displaying the results. There are three graphs, indicating the received signal IQ components for each channel, the baseband power spectrum showing the appropriate frequency detected 1.6 kHz bandwidth for each channel and the Music Detection Peak.

- Receiver VI Block Diagram

The actual programming for the receiver implementation is done in the LabVIEW block diagram. The idea is to run the algorithms for a large number of loops in order to get reliable test results. As there are two different algorithms used in this project, a processing Algorithms for Bartlett and Music using Matlab Script then LabVIEW functions.



Figure 3.31: USRP control Block

The block diagram of USRP control block is shown in Figure 3.32. The upper part is an interface between the front panel and the block diagram. It receives the USRP parameters provided by user from the front panel and sends them to the built in USRP control functions. The lower part shows the built-in USRP control functions and the connections in the implementation. The USRP device name is selected and sent to NI-USRP RX Open Session function(I), this function is used to start connections between LabVIEW VI and the USRP hardware, and this function also creates a handle of the USRP device. All the USRP control functions connected with this handle operate the same USRP device. Then the user specified USRP parameters are sent to USRP Configure Signal function and USRP Initiative function (II and III), these two functions are used to initialize the USRP device with the user specified parameters such as carrier frequency, I/Q sampling rate, etc. The final function is the USRP RX Fetch function (IV), this function is the function actually fetching data from the receiver antenna. The received data is then transmitted as the raw data. It is obvious that the data flow in LabVIEW block diagram is from left to the right, and the functions on the left executes first.

As seen in Figure 3.32, the raw data from NI-USRP RX Fetch function is then sent to a series of baseband signal processing blocks (1, 2, 3, 4). The first block is IQ graph, in order to display the received signals, as mentioned before. The frequency of the received signals is checked using baseband power spectrum that is shown in block 2. The signal is then calibrated in phase (3), in order to overcome the Phase synchronisation problem mentioned before. are then merged again to form the processed complex signal. The USRP stop and USRP close session function are seen in this figure.

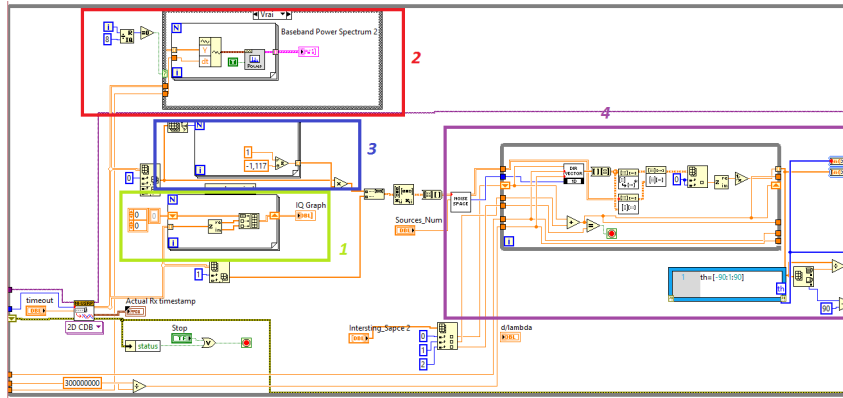


Figure 3.32: Block diagram of baseband signal processing

Algorithms implemented using MatLab integrated with LabVIEW

Implementation of MuSiC and Bartlett Algorithms with Matlab integrated in LabVIEW successfully works. Thus we achieve to localize precisely the Angle of Arrival. However, a Buffer overflow occurs during the execution of the algorithm due to the time of launching MatLAB software and integrate it into Labview environment

Music Algorithm / Bartlett Algorithm :

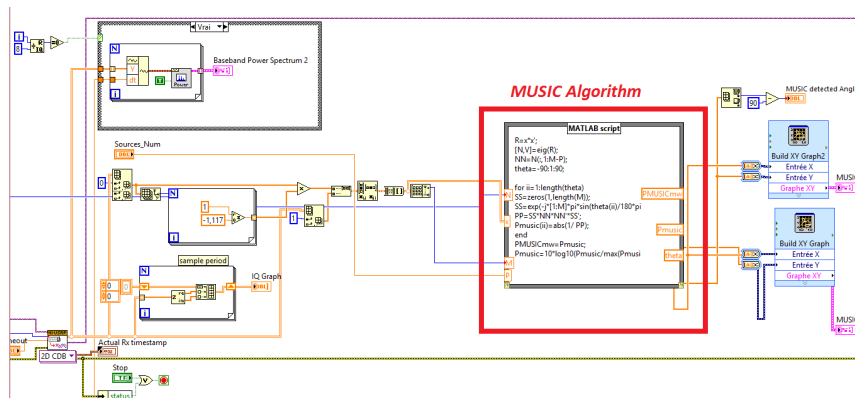


Figure 3.33: Implementation of Music Algorithm with Matlab block diagram

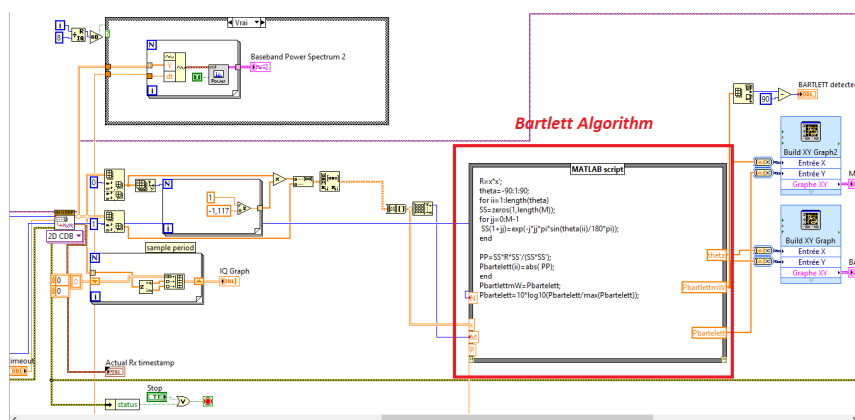


Figure 3.34: Implementation of Bartlett Algorithm with Matlab block diagram

Algorithms implemented using LabVIEW Functions

In this work, we define a new implementation of MuSiC and Bartlett algorithms by converting each operation, function and manipulation into LabVIEW functions already defined. Thus, we gained Real Time and optimisation. Therefore, Detection peak of angle of Arrival works precisely. in the following screen shots are presented MuSiC and Bartlett Algorithms.

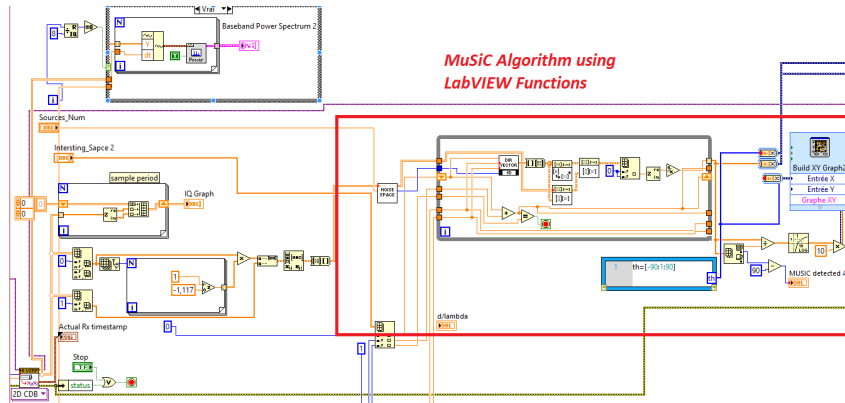


Figure 3.35: Implementation of MuSiC Algorithm using LabVIEW Functions

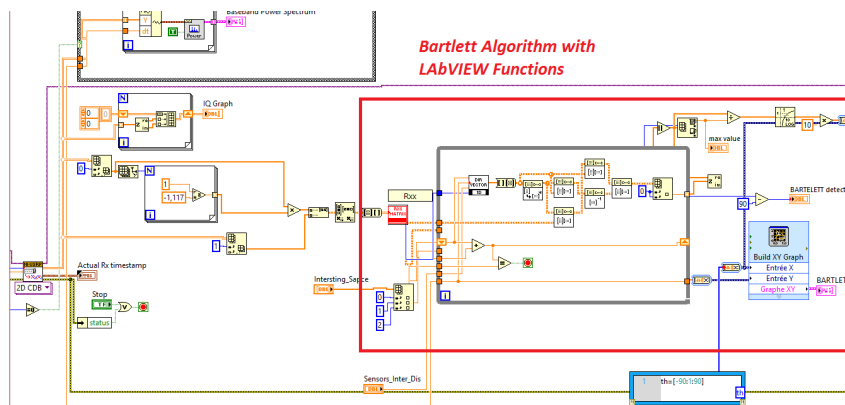


Figure 3.36: Implementation of Bartlett Algorithm using LabVIEW Functions

Chapter 4

Localization Results and Discussions

The performance of MUSIC and BARTLETT algorithms depends on following parameters :

1. Number of snapshots.
2. Array element spacing.
3. SNR (signal noise ratio).

While implementing MUSIC and BARTLETT Algorithms we observed two unpleasant phenomena:

1. Broadside.
2. Multipath.

4.1 Results of Implementation MuSiC and Bartlett Algorithms

4.1.1 Effect of the Number of Snapshots on MuSiC and Bartlett Algorithms

The first implementation results show how a signal is recognized by the MUSIC algorithm. There is a narrow band signal, the incident angle is -10° , this signal is not correlated, the noise is ideal Gaussian white noise, the SNR is 0 dB, the element spacing is half of the input signal wavelength, array element number is 2, the number of snapshots is 10, 200 and 16384. The results are shown in(Figures : 4.1, 4.2 and 4.3).

For relationship between MUSIC algorithm and the number of snapshots As can be seen from (Figures : 4.1, 4.2 and 4.3),

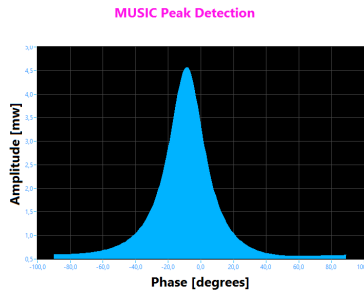


Figure 4.1: MuSiC with 10 snapshots

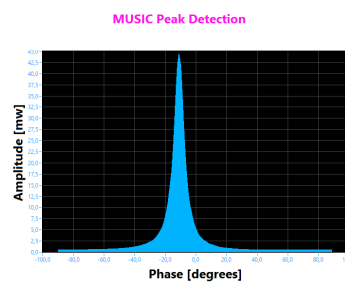


Figure 4.2: MuSiC with 200 snapshots

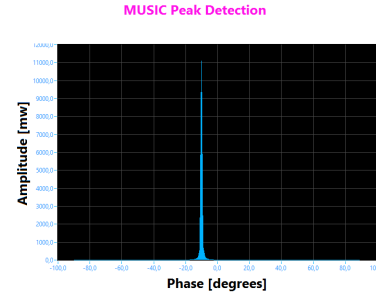


Figure 4.3: MuSiC with 16384 snapshots

With the other conditions remaining unchanged and with the increase in the number of snapshots, the beam width of DOA estimation spectrum becomes narrow, the direction of the array element becomes good and the accuracy of MUSIC algorithm is also increased.

Hence, the number of sample snapshots can be expanded to multiply the accuracy of DOA estimation, but the more sample snapshots, the more the data needs to be processed; the more amount of calculation of MUSIC algorithm, the lower the speed. So in practical application, we select reasonable sampling snapshots which ensure the accuracy of DOA estimation, minimize the amount of computation and accelerating the speed of work and saving resources. This is why we selected 16384 samples/ Fetch. While, BARTLETT resolution does not change increasing the number of snapshots, as illustrated in (Figures : 4.4, 4.5 and 4.6).

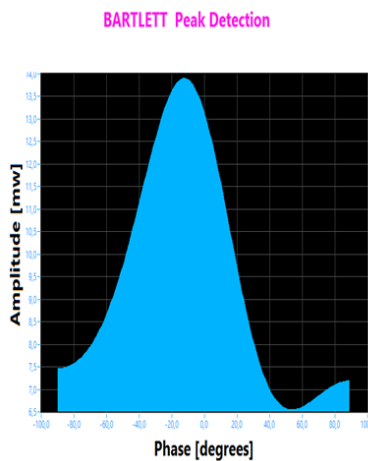


Figure 4.4: Bartlett 10 snapshots

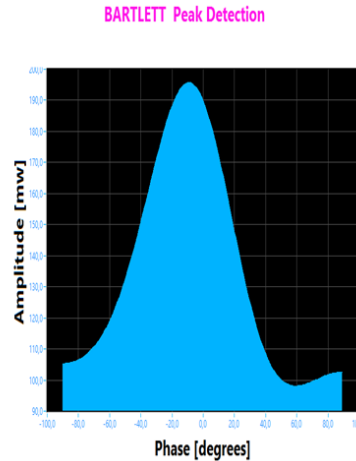


Figure 4.5: Bartlett 200 snapshots

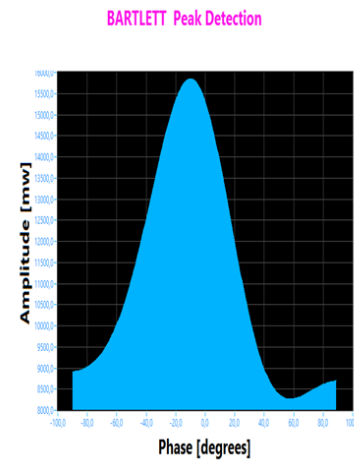


Figure 4.6: Bartlett 16384 snapshots

4.1.2 Effect of the Varying array spacing on MuSiC and Bartlett Algorithms

In this test, keeping all parameters constant and for the array spacing is ($d=\lambda$), ($d=\lambda/2$) and ($d=\lambda/4$).The results for MuSiC Algorithm are shown in Figures : (4.7, 4.8 and 4.9).

With the other conditions remaining the same, when the array element spacing is not

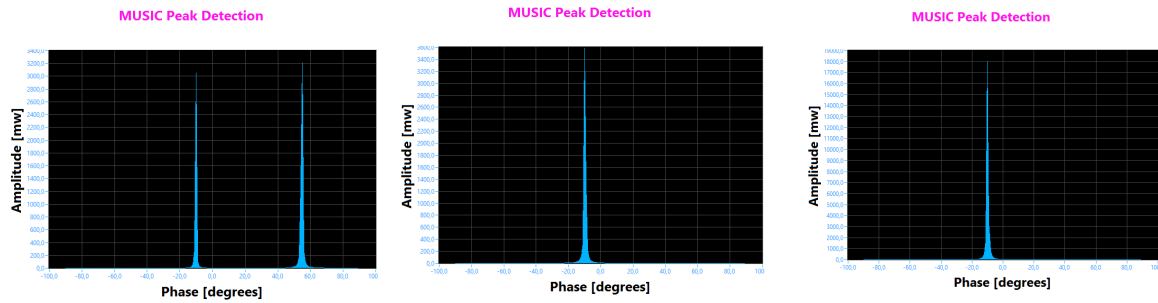


Figure 4.7: MuSiC ($d=\lambda$) Figure 4.8: MuSiC ($d=\lambda/2$) Figure 4.9: MuSiC ($d=\lambda/4$)

more than half the wavelength, with increasing array element spacing, the beam width of DOA estimation spectrum becomes narrow, the direction of the array elements becomes good;

that is to say, the resolution of MUSIC algorithm improves with the increase in the spacing of array element.

But, when the spacing of the array elements is larger than half the wavelength, the estimated spectrum, except for the signal source direction, shows false peaks, so it has lost the estimation accuracy.

Hence, in practical applications, more attention should be paid to the spacing of the array elements; element spacing can be increased but must not exceed half the wavelength, which is a very important point. It is best to set half the wavelength element spacing. Yet, BARTLETT algorithm resolution is not affected by the inter array elements distance as can be seen in (Figures : 4.10, 4.11 and 4.12).

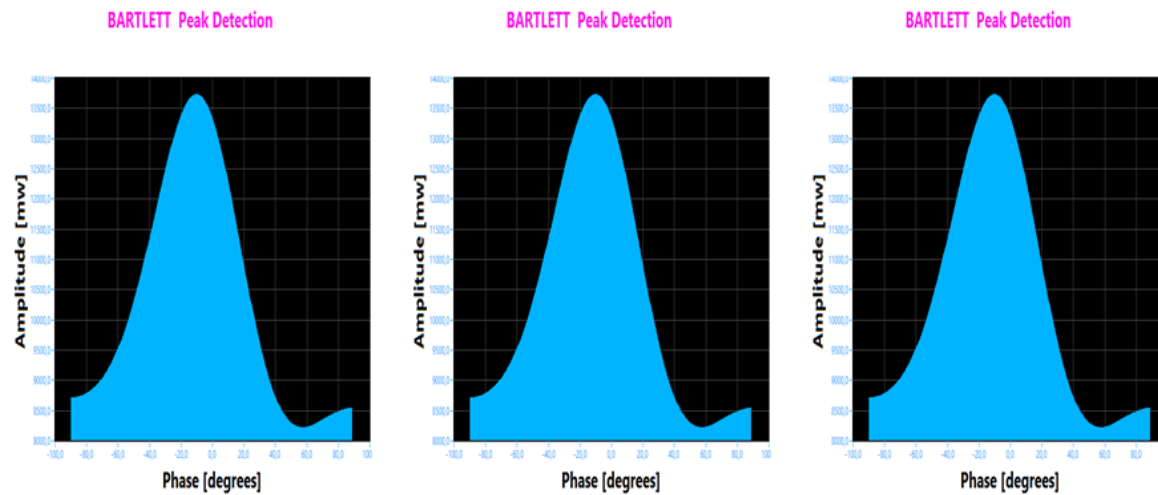


Figure 4.10: BARTLETT ($d=\lambda$) Figure 4.11: BARTLETT ($d=\lambda/2$) Figure 4.12: Bartlett ($d=\lambda/4$)

4.1.3 Effect of the SNR on MuSiC and Bartlett Algorithms

All other simulation parameters are kept constant and if the SNR is increased the direction of signal becomes clearer than and accuracy of MUSIC algorithm improves. The spectrum of DOA estimation becomes narrow.

For the relationship between MUSIC algorithm and SNR. As can be seen from (Figures : 4.13, 4.14 and 4.15). With the other conditions remainin unchanged, with the increase in the number of SNR, the beam width of DOA estimation spectrum becomes narrow, the direction of the signal becomes clearer, and the accuracy of MUSIC algorithm is also increased.

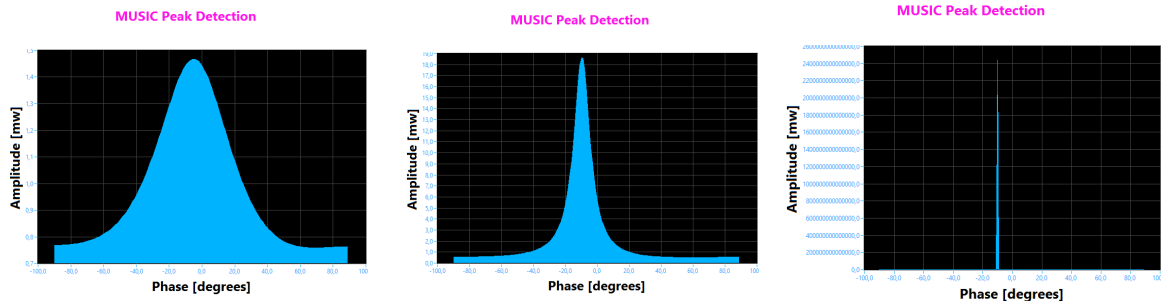


Figure 4.13: MuSiC SNR=20dB
Figure 4.14: MuSiC SNR=10dB
Figure 4.15: MuSiC SNR=0 dB

The value of SNR can affect the performance of high resolution DOA estimation algorithm directly. At low SNR, the performance of MUSIC algorithm will sharply decline, thus, improving the estimation performance under low SNR is a main research topic for high resolution DOA estimation. The signal subspace and orthogonal noise subspace are estimated, and then the spatial spectrum is constructed to achieve DOA estimation. The accuracy of DOA estimation under low SNR has large room for development and improvement, pending further study. Where, BARTLETT can not be changed by varying SNR. As shown in (Figures : 4.16, 4.17 and 4.18).

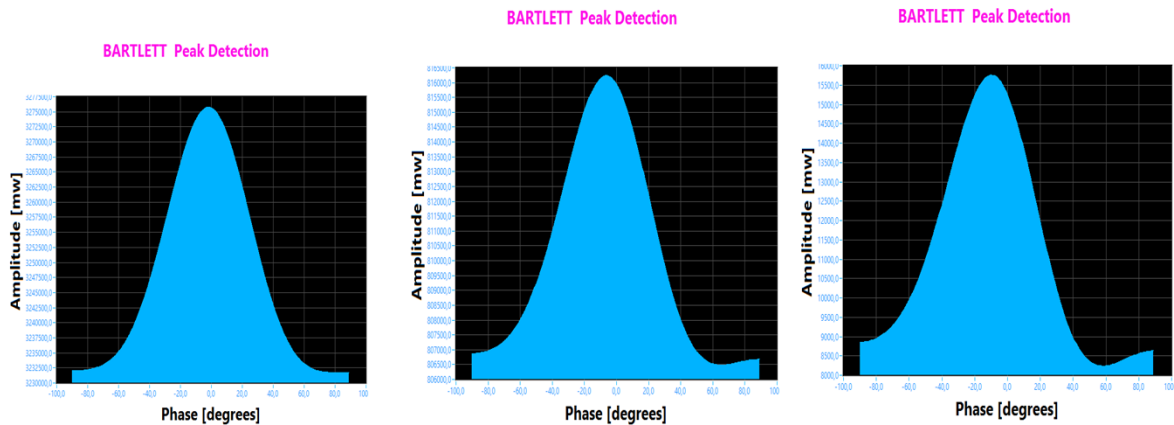


Figure 4.16: Bartlett SNR=20dB
Figure 4.17: Bartlett SNR=10dB
Figure 4.18: Bartlett SNR=0dB

4.2 Effect of the Broadside phenomenon on MuSiC and Bartlett Algorithms

In both of the implemented algorithms we noticed that when we get closer to the broadside angles from -90 degrees to -67 degrees and 67 degrees to 90 degrees we get 2 beams

instead of the beam according to the arrival angle. In the following figures (Figures : 4.19, 4.20 and 4.21 and 4.22, 4.23 and 4.24) show the Broadside angles effect on MuSiC and BARTLETT algorithms respectively.

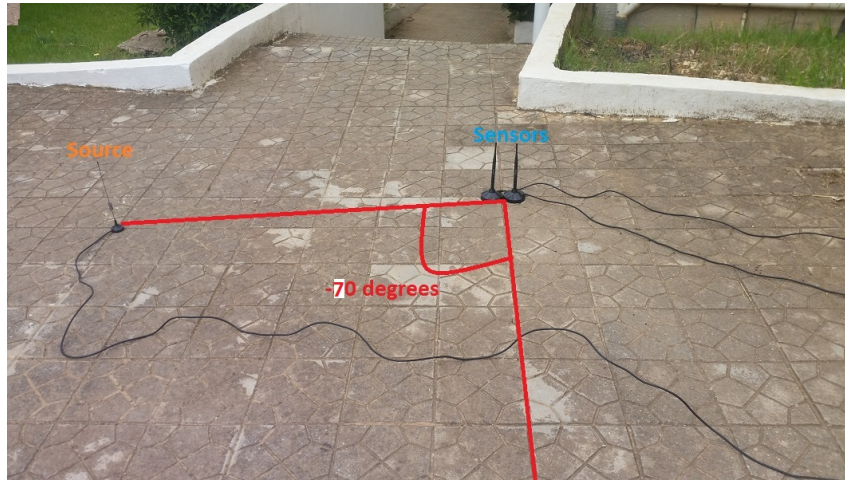


Figure 4.19: Broadside -70 degrees

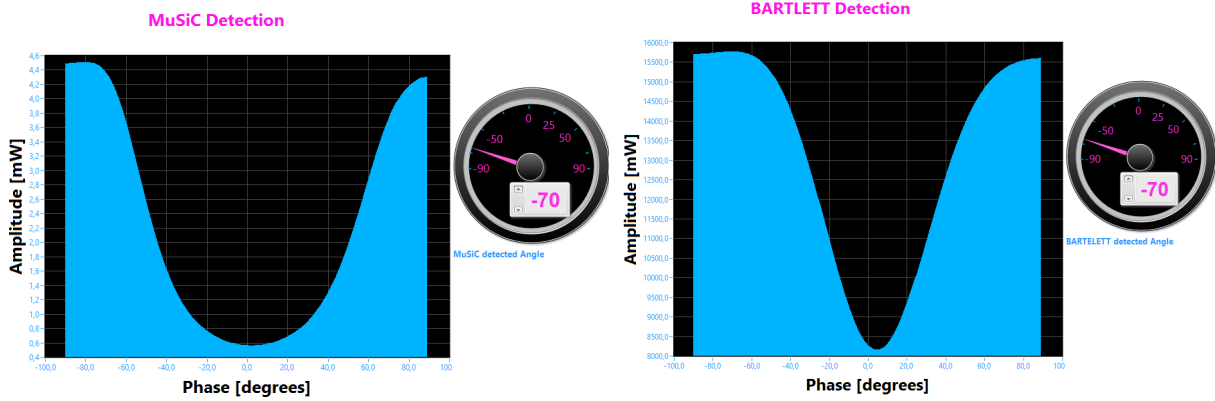


Figure 4.20: MUSIC broadside -70

Figure 4.21: Bartlett broadside -70

4.3 Effect of the Multipath phenomenon on MuSiC and Bartlett Algorithms

The received signal propagated over the radio is made not only from the signal that comes directly from the transmitter but also from the combination of reflected, diffracted and scattered copies of the original one. This effect is known as multi-path propagation.

Multipath signal is often considered an interference that must be removed. The coherence between multipath and direct component makes it difficult to use conventional direction-of arrival (DOA) estimation methods in a smart antenna system, So many studies and research are working to fix this problem, in our project We opted to verify this phenomena this is why we performed several indoor and outdoor tests. Thus, in outdoor tests we get a more stable and accurate detection peak rather than indoor test.

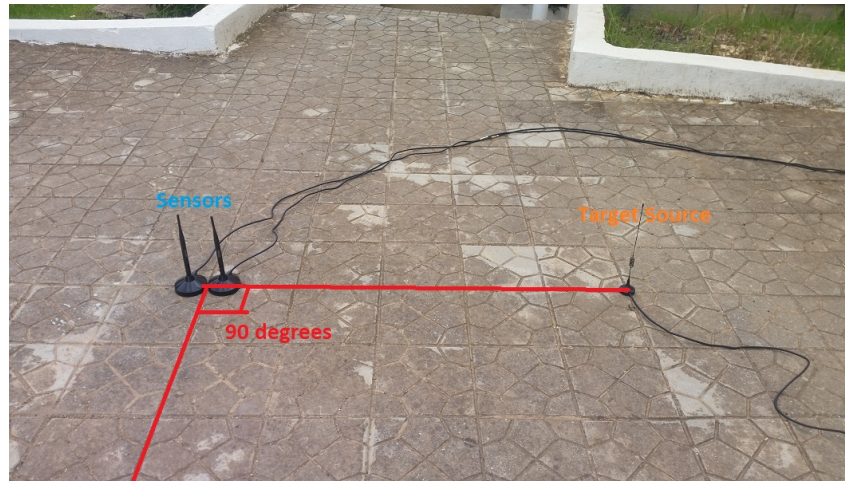


Figure 4.22: broadside angle 90 degrees

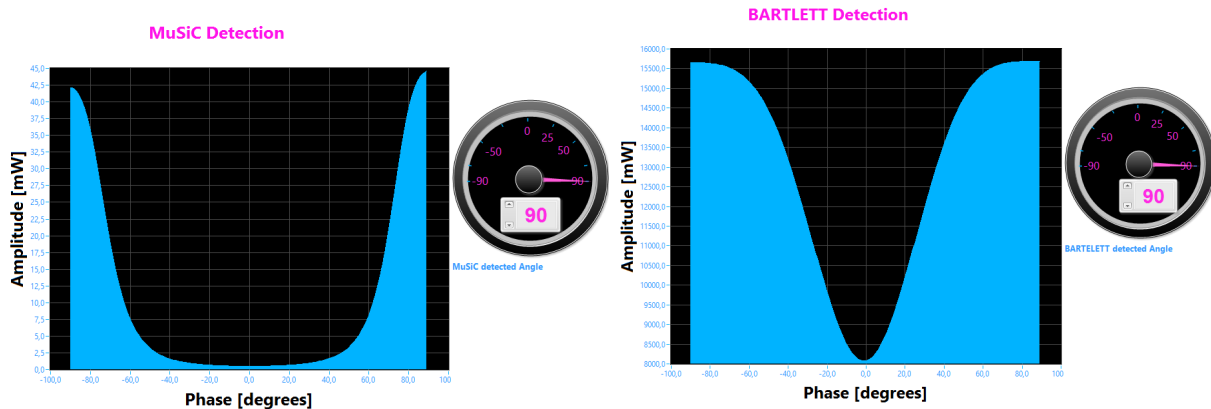


Figure 4.23: MUSIC broadside 90

Figure 4.24: Bartlett broadside 90

4.4 Indoor and Outdoor environment tests

The performance of the DOA estimator is verified by conducting experiments for a couple of test cases in an open atmosphere and indoor tests for a single source placed at arbitrarily selected angles from the array reference.

4.4.1 Indoor environment test

A single RF source is placed in the far-field region of a ULA at different angles from the array reference. The middle between array spacing receiver antennas of the ULA is considered as an array reference. The experimental configuration for the first case is shown in Figure (Figures : 4.25, 4.26 and 4.27 and 4.28, 4.29 and 4.30).

4.4.2 Outdoor environment test

The experimental results of MUSIC and BARTLETT algorithms for several angles of source are shown in Figure (4.34 , 4.31). The figures (4.35 , 4.32 , 4.36 and 4.33) shows

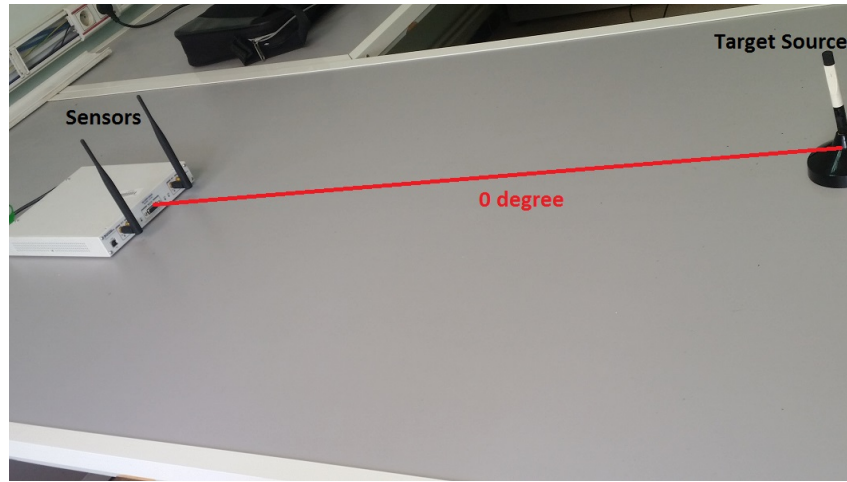


Figure 4.25: Indoor test 0 degree

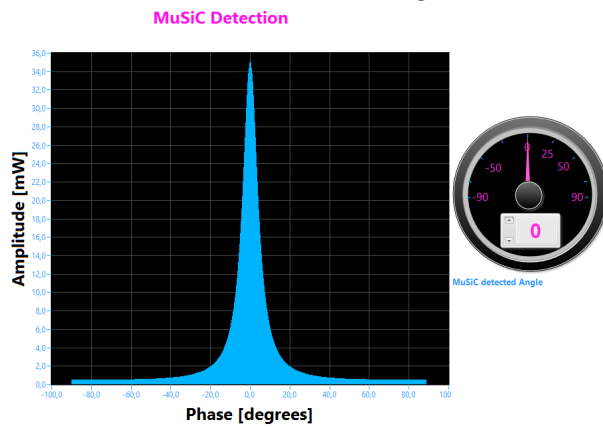


Figure 4.26: MuSiC indoor detection 0

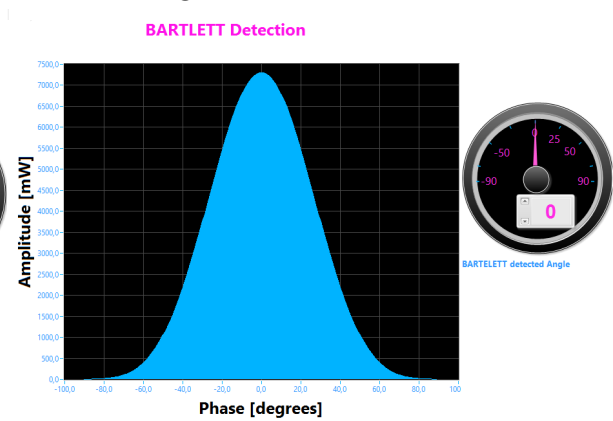


Figure 4.27: Bartlett indoor detection 0

the estimated DOAs of -45 degrees and 0 degrees respectively. In order to confirm the experimental angles, the source angle is also measured manually with a protractor and a string extended from the source antenna to the reference antenna of the ULA. The manually measured source angle is 0 and -45 respectively indicates close experimental estimates obtained with the implemented algorithms.

The experimental results for test cases are presented for a single RF sources lying at arbitrarily selected angles. The results indicate successful real time implementation of MuSiC and BARTLETT algorithms.

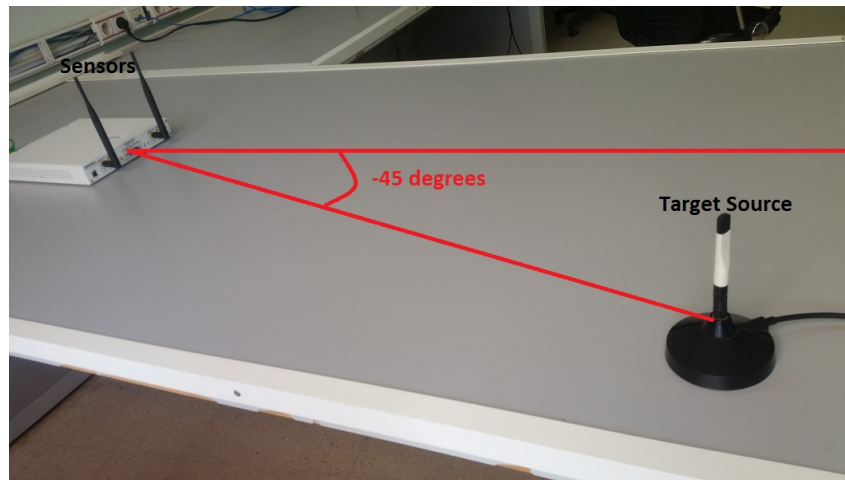


Figure 4.28: Indoor test -45 degree

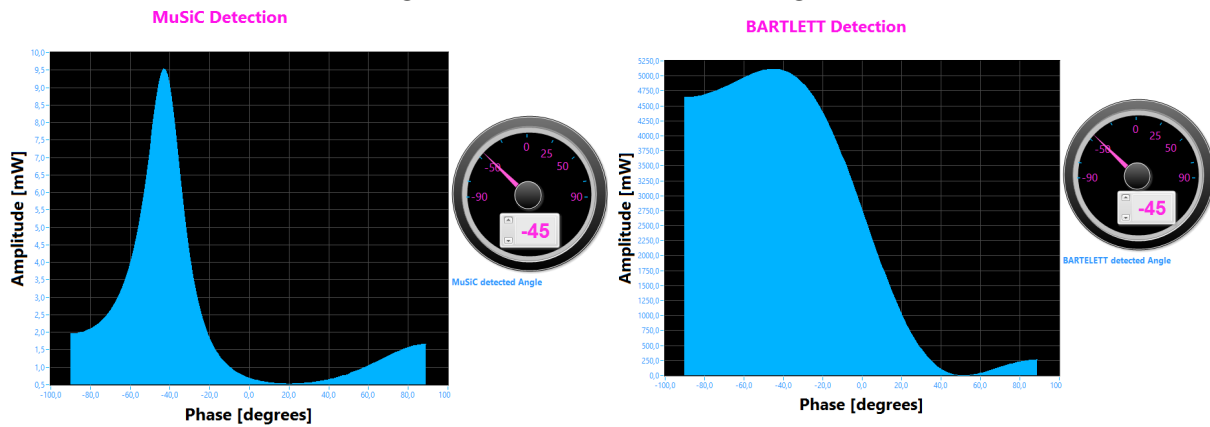


Figure 4.29: MuSiC indoor detection -45

Figure 4.30: Bartlett indoor detection -45

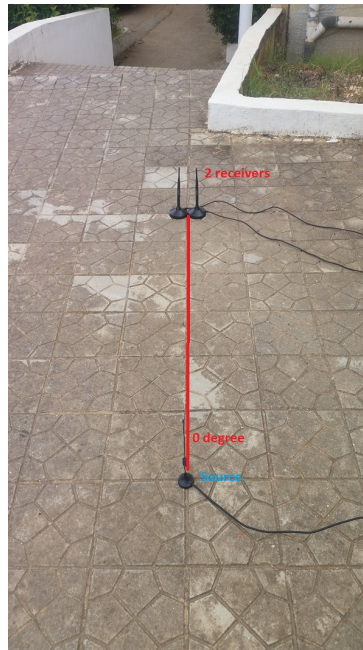


Figure 4.31: Outdoor test
0 degrees

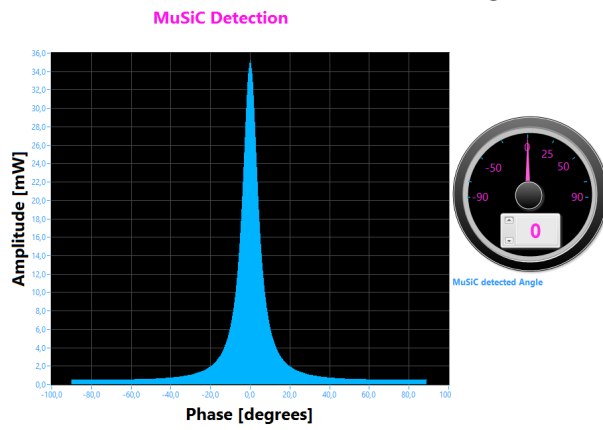


Figure 4.32: MuSiC indoor detection 0

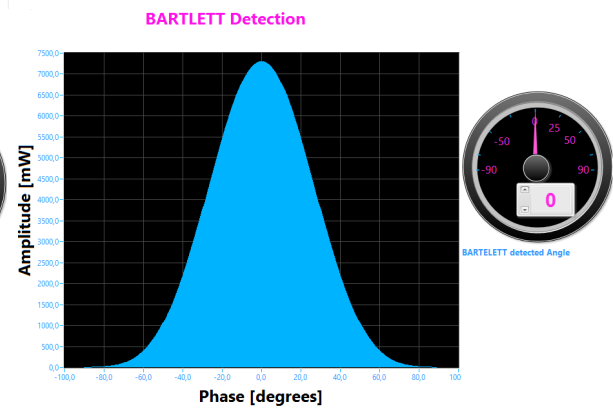


Figure 4.33: Bartlett indoor detection 0

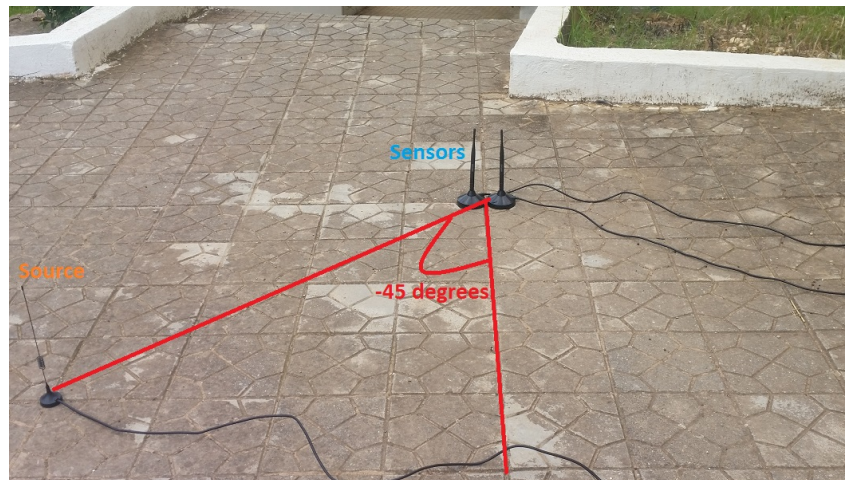


Figure 4.34: Outdoor test -45 degrees

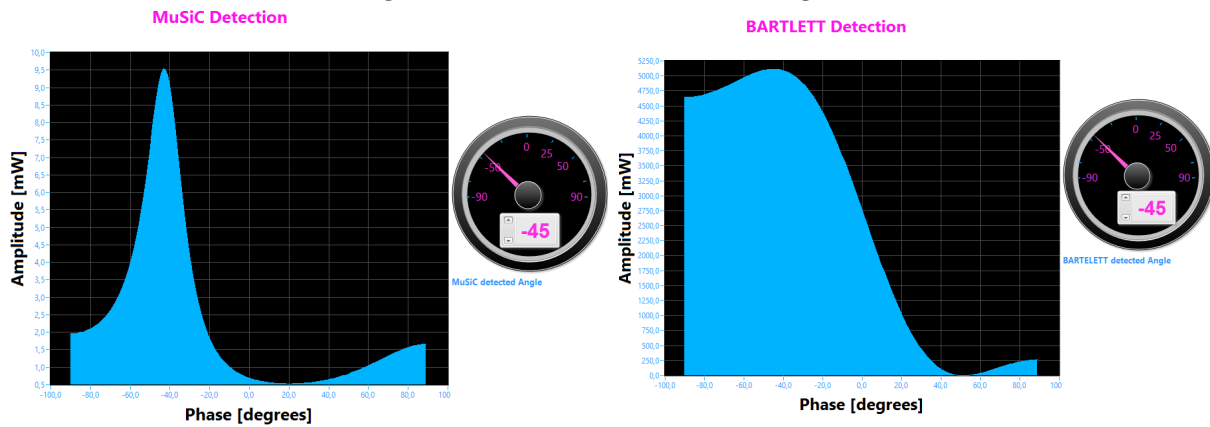


Figure 4.35: MuSiC indoor detection -45

Figure 4.36: Bartlett indoor detection -45

Conclusion

Many skills were developed during this challenging project making use of information learned in the Digital Telecommunication and Signal Processing courses.

The ultimate aim of this project was to implement Localization Algorithms based on DOA theory using NI USRP hardware devices and NI LabVIEW platform in realistic environment under normal conditions.

The primary goal of this thesis was realized. A flexible test bed environment was developed and used to analyse the performance of a smart antenna system. Test results were collected and used to analyse the performance of DOA estimation and beamforming. Software defined radio is a very good technology that array signal processing can benefit from. The work exerted in this project has paved the way for faster future progress in the research group.

The synchronisation of the USRP boards and USRP RIO channels made the problem of the phase uncertainty less severe, because solving the phase problem in the hardware and separating it from the RF stage (Antenna array) enables easier investigation of the error source. Even though the project was not mainly concerned about calibration, it turned out that the most critical issue in the testbed operation is the calibration. After observing the project results and the following discussions in the previous chapter, it can be said that BARTLETT and MUSIC algorithms are very sensitive to array uncertainties and environment. There are many uncertainties need to be estimated by careful array calibration before both of the algorithms will be successful.

There are still many things that can be done on this project in the future so that the system works better, We would suggest the following points:

1. Implementing more advanced and automated calibration algorithms. Manual phase calibration has proved to be insufficient for practical systems.
2. Working in a lab with more space and less obstacles will enhance the environment and hence, enhance the performance.
3. Although there are 4 USRP boards and 4 RIO USRP boards available in the lab; only one USRP board and a RIO USRP were used because the number of computer

PICe ports is limited to just one. Using 2 elements in an array is not enough for good BARTLETT and MUSIC results. Future work may consider using more elements if the location uncertainty is handled. Hence We have opted to set up a hybride Receiving System including of NI USRP and Rio USRP in order to increase number of the array elements up to 3 elements.

Bibliography

- [1] Hands-On: Introduction to Software Defined Radio with NI USRP, www.Hands-On: Introduction to Software Defined Radio with NI USRP.com ,2013.
- [2] author=Sun, Chen and Karmakar, Nemaï Chandra, Direction of arrival estimation based on a single port smart antenna using MUSIC algorithm with periodic signals, pages=153–162, year=2004
- [3] author=Sharma, Bindu and Singh, Ghanshyam and Sarkar, Study of DOA estimation using music algorithm, pages=594–603, year=2015
- [4] author=Fistas, Nikolaos and Manikas, A new general global array calibration method, pages=IV–73, year=1994, organization=IEEE
- [5] author=Amin, Md Shahedul and Azim, Md Riyasat and Rahman, Syed Prantik and Habib, Ferdous and Hoque, Ashraful, Estimation of Direction of Arrival (DOA) using real-time array signal processing and performance analysis, journal=IJCSNS, year=2010
- [6] author=Naderi Shahi, Sina and Emadi, Mohammad and Sadeghi, KH, High resolution DOA estimation in fully coherent environments, pages=135–148, year=2008, EMW Publishing
- [7] author=Tayem, Nizar and Raza, Syed Ahmed and Omer, Muhammad and El-Lakki, Mohamed and Nayfeh, Jamal F, Hardware implementation of a proposed Qr-Tls DOA estimation method and Music, ESPRIT Algorithms on Ni-Pxi platform, pages=203–221, year=2013,
- [8] author=Gao, Yan and Chang, Wenjing and Pei, Zeng and Wu, Zhengjiang, An improved music algorithm for DOA estimation of coherent signals, year=2014, publisher=IFSA Publishing, SL
- [9] author=Pradyumna Vasudeo Desale, SOFTWARE DEFINED RADIO BASED ANGLE OF ARRIVAL FOR FIRST-RESPONDER SCENARIOS, year=2014, publisher=Thesis in Electrical Engineering ,May 2010,EMW Publishing
- [10] author= Ahmad, Mushtaq and Zhang, Xiaofei, Performance of MUSIC Algorithm for DOA Estimation,ICAYS Engineering Mechanics and Interdisciplinary, year=2016,
- [11] author=Zheng, Zhenyu , Experimental Evaluation of Spectrum Sensing Algorithms for Wireless Microphone Signal, year=2014.
- [12] author= Nehete, Viraj Dileep,nehete , Experimental evaluation of 2 x 2 MIMO in LOS and NLOS channels using NI USRP-2953R, year=2016.

-
- [13] author=Sun, Chen and Karmakar, Nemai Chandra, Direction of arrival estimation based on a single port smart antenna using MUSIC algorithm with periodic signalsInternational, pages=153–162, year=2004.
- [14] author=Mao, Shiwen and Huang, Yingsong and Li, Yihan and Agrawal, Prathima and Tugnait, Jitendra, Introducing software defined radio into undergraduate wireless engineering curriculum through a hands-on approach,Proc, pages=1–10, year=2013.
- [15] Hands-On: Introduction to Software Defined Radio with NI USRP,www.Hands-On: Introduction to Software Defined Radio with NI USRP.com ,2013.
- [16] author=Mitola III, Joseph, Software radio architecture: object-oriented approaches to wireless systems engineering, pages=1–10, year=2004.
- [17] author= Abu-Shaban, Zohair M, Localisation Testbed using Software-Defined Radio, year=2010, publisher=London-United Kingdom: Imperial College London